



**HAL**  
open science

## Salphen-Co(III) complexes catalyzed copolymerization of epoxides with CO<sub>2</sub>

Zdeněk Hošťálek, Robert Mundil, Ivana Císařová, Olga Trhlikova, Etienne Grau, Frédéric Peruch, Henri Cramail, Jan Merna

► **To cite this version:**

Zdeněk Hošťálek, Robert Mundil, Ivana Císařová, Olga Trhlikova, Etienne Grau, et al.. Salphen-Co(III) complexes catalyzed copolymerization of epoxides with CO<sub>2</sub>. *Polymer*, 2015, 63, pp.52-61. 10.1016/j.polymer.2015.02.018 . hal-01365295

**HAL Id: hal-01365295**

**<https://hal.science/hal-01365295>**

Submitted on 26 Nov 2019

**HAL** is a multi-disciplinary open access archive for the deposit and dissemination of scientific research documents, whether they are published or not. The documents may come from teaching and research institutions in France or abroad, or from public or private research centers.

L'archive ouverte pluridisciplinaire **HAL**, est destinée au dépôt et à la diffusion de documents scientifiques de niveau recherche, publiés ou non, émanant des établissements d'enseignement et de recherche français ou étrangers, des laboratoires publics ou privés.

# Salphen-Co(III) complexes catalyzed copolymerization of epoxides with CO<sub>2</sub>

Zdeněk Hošťálek, Robert Mundil, Ivana Císařová, Olga Trhlíková, Etienne Grau, Frederic Peruch, Henri Cramail, Jan Merna

## Abstract

The series of novel symmetric and asymmetric salphen cobalt (III) complexes with different counteranions (trichloroacetate, dinitrophenolate, pentafluorobenzoate and acetate) was synthesized and used as catalysts in copolymerization of CO<sub>2</sub> with propylene oxide (PO) and cyclohexene oxide (CHO). Hexacoordinated structure of complexes adducts was found in solid phase. The effect of catalyst structure, temperature, CO<sub>2</sub> pressure, catalyst/cocatalyst ratio on overall activity and selectivity was investigated. Synthesized salphen-Co (III) complexes were effective for both PO/CO<sub>2</sub> and CHO/CO<sub>2</sub> highly alternating copolymerization. Substitution of phenylene framework of salphen ligand by chlorine atom led to decrease of activity in PO/CO<sub>2</sub> copolymerization. Complexes with trichloroacetate counteranion were shown to be the most active and selective in PO/CO<sub>2</sub> copolymerization leading to poly(propylenecarbonate) with highest molar mass. On contrary, catalytic performance of salphen Co (III) complexes in CHO/CO<sub>2</sub> copolymerization was almost independent on ligand structure and counteranion. Excellent selectivity to poly(cyclohexenecarbonate) was achieved even at 0.1 MPa CO<sub>2</sub>. MALDI-TOF analysis of polycarbonates was used to investigate the initiation step of the copolymerization.

## 1. Introduction

The use of CO<sub>2</sub> as a C1 feedstock in chemical synthesis became an attractive research target, since it is abundant, renewable and nontoxic gas [1], [2]. Beside classical large scale industrial processes like urea manufacture, CO<sub>2</sub> could find an application also as a substrate for synthetic polymer production, thus reducing the dependence of their production on crude-oil. A great interest was devoted especially to copolymerization of epoxides with CO<sub>2</sub>, which represent a new, phosgene free, route towards aliphatic polycarbonates. The versatility of this synthetic approach lies in possibility to prepare polyesters with very different properties by variation of the epoxide structure.

Although the first catalytic system used for copolymerization of epoxides with CO<sub>2</sub> (heterogeneous ZnEt<sub>2</sub>/H<sub>2</sub>O) was reported already in 1969 [3], the significant progress in field of CO<sub>2</sub> polymer chemistry was achieved in last decade, when new types of homogenous catalytic systems were discovered [4], [5]. Variety of metal complexes of zinc [6], [7], [8], cobalt [9], [10], chromium [11], [12], [13], magnesium [14], manganese [15], aluminium [16], iron [17], [18] and rare-earth metals [19], [20], [21] proved to be effective for epoxide/CO<sub>2</sub> copolymerization. Prominent among these catalysts are  $\beta$ -diiminate zinc complexes [8] and metal salen complexes [22], which show high activity, selectivity to polycarbonate, good stereoselectivity and in some cases enhanced

enantioselectivity [23], [24], [25] at mild conditions. So far, a large number of salen catalysts was prepared by complexation of salen ligands mostly with Al, Cr and Co precursors. These complexes efficiently catalyzed coupling of epoxides with CO<sub>2</sub> to produce cyclic carbonates or polycarbonates. The most effective catalysts for epoxide/CO<sub>2</sub> copolymerization proved to be chiral salen Co (III) complexes in combination with strong Lewis acids and nucleophilic cocatalysts [22].

Since 2003, when Coates first reported salen Co(III) complex [10] which showed an excellent selectivity to poly(propylenecarbonate) (PPC) formation (99% vs. cyclic carbonate) with 99% of carbonate linkages, a significant effort was devoted to the synthesis of more efficient salen Co complexes as well as mechanistic studies, which contributed to better understanding of reaction mechanism [24], [26], [27]. Based on the number of metal atoms involved in the catalytic cycle, monometallic or bimetallic mechanisms have been described [28]. A detailed study of salen Co (III) complexes with various ligand substitutions, initiating groups and cocatalysts was performed by Lu and coworkers [23]. It was concluded, that ideal catalytic system for epoxide/CO<sub>2</sub> copolymerization is chiral (R,R')-Salen Co (III) complex with *tert*-butyl substituents in ortho and para positions of aryl rings in salen ligand. Further, low nucleophilicity of initiating group is crucial for high catalyst activity as well as the use of cocatalyst (ionic salt with bulky cation) with poor leaving group [23], [29]. Significant increase in activity was achieved when novel types of single component salen Co(III) catalyst with covalently attached cocatalyst groups (ammonium) were synthesized [30], [31]. These complexes show very high activities up to 26,000 h<sup>-1</sup> at low catalyst loadings (1:100,000) and elevated temperatures (80 °C) compared to activity in order of 10<sup>2</sup> h<sup>-1</sup> displayed by simple salen complexes [23], [32]. Similarly, Co complex with 1,5,7-triazabicyclo[4,4,0] dec-5-ene (TBD) side arm showed very high TOF 10,800 h<sup>-1</sup> and high molar mass up to 100 kg mol<sup>-1</sup> [33]. However, high catalytic activity of these complexes is paid by a tedious multistep procedure of their preparation.

For the synthesis of stereoregular polycarbonates catalytic systems with enhanced stereoselectivity were developed [34], [35]. Beside simple already discussed chiral salen Co complexes, which can afford enantioenriched polycarbonates (kinetic resolution of epoxide enantiomers with  $k_{rel}$  up to 9.7) [24], the significantly higher  $k_{rel}$  value (or enantiomeric excess) was achieved with multichiral [36], [37] and bimetallic bridged [38] salen Co(III) complexes to produce more enantioenriched PPC and poly(cyclohexenecarbonate) (PCHC) respectively. Enantioselectivity of salen complexes in copolymerization of propylene oxide (PO) with CO<sub>2</sub> was investigated in detail and related to the bimetallic or binary mechanism of copolymerization [39].

An extensive research was devoted to CO<sub>2</sub> with epoxide copolymerizations catalyzed by salen complexes with chiral (R,R') cyclohexylene backbone [22] while only few publication was devoted to its salphen analogues containing phenylene ligand backbone (Fig. 1). Compared to salen analogues salphen ligands are more cost-effective, their substitution is more feasible and their rigid geometry allows to efficiently influence the Lewis acidity of the metal center and subsequently the reactivity of the corresponding complex [40]. Indeed, some salphen complexes proved to be effective catalysts for various types of substrates (carbonylation, epoxidation,

epoxide and lactones ROP) and, in some cases, they exceeded their salen analogues [11], [41], [42], [43], [44], [45]. First copolymerization of PO with CO<sub>2</sub> catalyzed by salen chromium complex in combination with 4-dimethylaminopyridine (DMAP) cocatalyst was performed by Rieger in 2003 [11] resulting in a mixture of cyclic propylenecarbonate (CPC) and PPC with  $M_n$  of 15 kg mol<sup>-1</sup>. A series of aluminium salen complexes was also used for copolymerization of cyclohexene oxide (CHO) with CO<sub>2</sub> to produce polycarbonates with  $M_n$  up to 10 kg mol<sup>-1</sup> and carbonate linkage up to 97% [42]. Copolymerization of PO with CO<sub>2</sub> was investigated using salen Co(III)Br complex without any cocatalyst resulting in high selectivity to PPC (99%) but poor activity (23 h<sup>-1</sup>) [24]. The same complex was reported as inactive for CHO/CO<sub>2</sub> copolymerization [46]. A monometallic and bimetallic flexibly linked salen chromium complexes were used in CO<sub>2</sub>/epoxide copolymerization producing selectively PPC with moderate TOF 50–90 h<sup>-1</sup> containing 40–90% carbonate linkage and  $M_n$  up to 32 kg mol<sup>-1</sup> [47]. Kinetic investigation proved the action of bimetallic mechanism (without cocatalyst) and binary (or monometallic) mechanism (with cocatalyst). Very recently the new salen Ti(III) complex was used for production of 100% alternating PCHC ( $M_n \approx 5$  kg mol<sup>-1</sup>) with TOF up to 570 h<sup>-1</sup> [48].

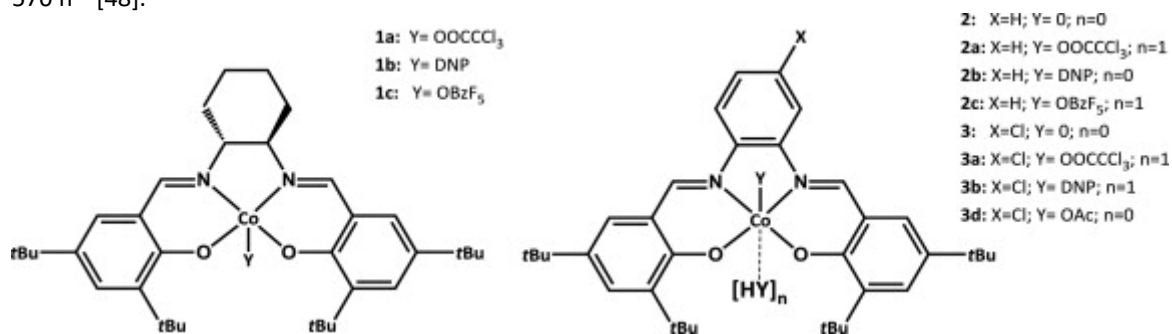


Fig. 1. Structure of chiral (R,R') salen complexes **1a–c** and prepared salen complexes (**2a–c,3a–d**).

Herein, we describe the synthesis of novel symmetric and asymmetric salen cobalt (III) complexes with different counteranions, and their reactivity in copolymerization of CO<sub>2</sub> with PO and CHO in presence of bis(triphenylphosphine)iminium chloride (PPNCl) as a cocatalyst. The effect of catalyst structure as well as of temperature, catalyst and cocatalyst loading on catalyst activity and selectivity was investigated.

## 2. Results and discussion

### 2.1. Preparation and characterization of Salphen Co(III) complexes

We synthesized a series of novel salen Co(III) complexes with trichloroacetate (O<sub>3</sub>CCl<sub>3</sub>), dinitrophenolate (DNP), pentafluorobenzoate (OBzF<sub>5</sub>) and acetate (OAc) counterions based on published procedure [23], by reacting ligands **L2** (N,N'-Bis(3,5-di-tert-butylsalicylidene)-1,2-phenylenediamine) and **L3** (N,N'-Bis(3,5-di-tert-butylsalicylidene)-4-chloro-1,2-phenylenediamine) with cobalt acetate and subsequent oxidation by oxygen in presence of nucleophile.

Prepared complexes were obtained in most of cases as microcrystalline dark red powders, unsuitable for solid state structure characterization. Crystals of Co(III) salen complexes bearing N,N'-Bis(3,5-di-tert-butylsalicylidene)-1,2-phenylenediamine ligand **L2** and OBzF<sub>5</sub> counteranion obtained by crystallization from CH<sub>2</sub>Cl<sub>2</sub>/hexane were suitable for X-ray analysis. Surprisingly the solid state structure shows that the complex is not an expected pentacoordinated complex with one OBzF<sub>5</sub> counteranion but a hexacoordinated octahedral complex bearing one OBzF<sub>5</sub> anion and another coordinated HOBzF<sub>5</sub> molecule (complex **2c**, Fig. 2). Although the other complexes could not be analyzed by X-Ray diffraction, we can deduce structure of complexes from elemental analysis (Table 1). Elemental composition of complexes **2b** and **3d** shows better agreement with structure calculated for salenCo(III) complex with one attached Y group, whereas complexes **2a**, **2b** and **3a** have probably hexacoordinated structure of YH adduct. Additional elemental analysis of hexacoordinated complex **2c** also confirms the presence two OBzF<sub>5</sub> groups. Non-integer values of average number of Y molecules coordinated to Co center shows that they are rather a mixture of pentacoordinated complexes and hexacoordinated YH adducts.

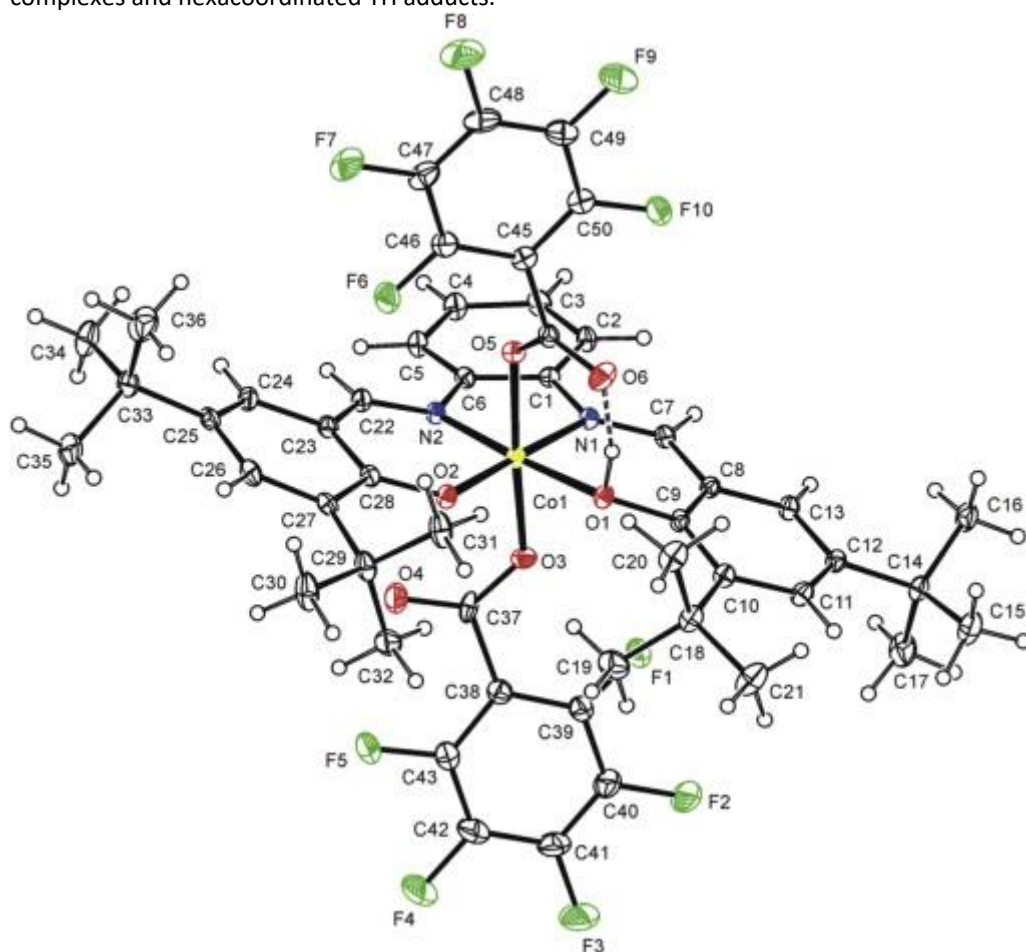


Fig. 2. View on the molecular structure of complex **2c** with atom numbering. The displacement ellipsoids are drawn on 30% probability level. The geometry is stabilized by short hydrogen bond: O(1)—H(1) ... O(6) 2.4418 (19) Å, angle at H(1) 165°.

Table 1. Elemental analysis of complexes **2a-c** and **2a,b,d**.

Complex		<b>2a</b>	<b>2b</b>	<b>2c</b>	<b>3a</b>	<b>3b</b>	<b>3d</b>
FOUND	C	53.93	65.53	60.00	50.01	58.40	65.43
	H	5.37	6.76	5.32	5.13	5.75	7.25
	N	3.28	6.28	2.89	2.81	6.37	4.18
Calculated for optimum	C	53.80	65.53	59.93	49.91	58.45	65.40
	H	7.76	6.50	4.79	4.70	5.28	6.95
	N	3.18	6.88	2.90	2.90	8.16	3.95
Optimum		1.75 eq.	0.85 eq.	1.75 eq.	2.05 eq.	1.80 eq.	1.30 eq.

NMR, FT-IR, HR-MS spectroscopy and elemental analysis were used for structural characterization of complexes. Both Salphen Co(III)<sup>+</sup> cation and Y<sup>-</sup> counteranion were detected for complexes **2b**, **2c** and also **3b** by HR-MS in positive and negative mode, respectively. Complexes **2a**, **3a** and **3d** were characterized only in HR-MS positive mode. Trichloroacetate group of complexes **2a** and **3a** attached to Co was confirmed by ATR-IR spectroscopy by observing typical vibration of C=O group at  $\approx 1700\text{ cm}^{-1}$ . Detailed COSY, HSQC and HMBC experiments were used to fully assign the <sup>1</sup>H and <sup>13</sup>C NMR spectra of new asymmetric salphen cobalt complex **3**. (See Fig. S4–8 in Supp. information).

## 2.2. Alternating copolymerization of propylene oxide and CO<sub>2</sub> with (salphen)CoY complexes

Basic salphen complex **2a** was used to optimize polymerization conditions (Table 2). PPnCl, the most frequent and efficient cocatalyst for salen complexes [23], [24], [32], [49] was used at 1:1 ratio to Co. At 1 MPa and ambient temperature **2a**/PPnCl affords a high molar mass polycarbonate with  $M_n$  25 kg.mol<sup>-1</sup>. However, the selectivity to polymer formation and TOF of **2a**/PPnCl are much lower compared to **1a**/PPnCl [23]. Lower activity of salphen complex **2a** compared to salen complex **1a** can be explained by stronger interaction of nucleophile Y group or growing polymer chain with Co center as a result of higher Lewis acidity of  $\pi$ -conjugated salphen complex. This limits ring-opening of activated epoxide molecules (during initiation and propagation step) by nucleophile which has to be released from Co center (in case nucleophile does not come from the cocatalyst). We could further expect that higher Lewis acidity of salphen complex should lead to better selectivity to polycarbonate vs. cyclic carbonate as was observed in the case of salphen Cr(III) complex compared to its salen analogue [11] However, in our case, the selectivity of salphen Co (III) complex **2a** to polycarbonate formation is lower at all conditions than in the case of benchmark salen complex **1a**. This shows on the complexity of the copolymerization reactions where many parameters play role and can work in opposite manner. Enhanced activity was observed at elevated temperature 50 °C and even at 75 °C. An optimal polymerization temperature of **2a** from point of view of both high TOF and selectivity to PPC (80%) was 50 °C. Decrease of selectivity to PPC

observed at higher temperatures is a general phenomenon of these catalytic systems due to higher activation energy for the formation of CPC than for the formation of PPC [29]. Decrease of pressure resulted in decrease of activity, molar mass and at 0.1 MPa also to significant decrease of selectivity to PPC (Exp. 3, 4, Table 2). However, even at 0.1 MPa polymer consists of more than 99% of carbonate linkage suggesting the insertion of CO<sub>2</sub> into metal-alkoxy bond is sufficiently fast.

Table 2. The effect of temperature and reaction pressure to *rac*PO/CO<sub>2</sub> copolymerization catalyzed by salphen Co complex **2a**/PPNCl.

Exp.	Cat.	<i>T</i> (°C)	<i>p</i> (MPa)	<i>t<sub>p</sub></i> (h)	<i>Y<sub>w</sub></i> POL <sup>a</sup> (%)	TOF <sub>POL</sub> <sup>b</sup> (h <sup>-1</sup> )	TOF <sub>CPC</sub> <sup>c</sup> (h <sup>-1</sup> )	<i>M<sub>n</sub></i> <sup>d,e</sup> (MALLS) (kg mol <sup>-1</sup> )	<i>D</i> <sup>d,e</sup>	Selectivity <sup>f</sup> (% PPC)
Ref [23]	<b>1a</b> <sup>g</sup>	25	1.5	1.5	–	568	–	30.9 <sup>h</sup>	1.20 <sup>h</sup>	99
1	<b>2a</b>	25	1	4	36.9	190	27	25.0(34 + 18)	1.09	88
2	<b>2a</b>	50	1	2	42.9	456	110	34.4(48 + 25)	1.16	81
3	<b>2a</b>	50	0.2	2	20.4	206	51	18.1(27 + 14)	1.13	80
4	<b>2a</b>	50	0.1	2	9.5	98	94	11.8(13 + 7)	1.24	51
5	<b>2a</b>	75	1	1	27.1	560	391	26.5(43 + 21)	1.25	59

Polymerizations run in neat epoxide, [PO]/[Co]/[PPNCl] = 2000:1:1; *V*<sub>PO</sub> = 1.5–2 mL; Carbonate linkage of all polymers were >99% as determined by <sup>1</sup>H NMR spectroscopy. a Based on isolated polymer yield. b Turnover frequency to polycarbonate. c Turnover frequency to cyclic carbonate; (For details see experimental part). d Determined by SEC-MALLS in THF. e All polymers exhibit bimodal distributions (values in brackets correspond to *M<sub>p</sub>*). f Selectivity to PPC over cyclic carbonate. g Ref. [23]: Chiral (R,R')SalenCo-OCCCCl<sub>3</sub> complex (Fig. 1). h Literature data, *M<sub>n</sub>* and *D* determined by SEC with PS standard calibration in THF.

Influence of catalyst/cocatalyst ratio on activity and selectivity to PPC was further investigated with **2a** combined with PPNCl (Fig. 3). Complex **2a** without PPNCl cocatalyst was almost completely inactive and produced only trace amount of CPC (TOF<sub>CPC</sub> ≈ 2 h<sup>-1</sup>) showing the crucial role of nucleophilic cocatalyst, which helps to ring opening of the epoxide as the rate determining step of the copolymerization. The highest activity, molar mass and maximum selectivity was observed at equimolar ratio of catalyst and cocatalyst. Further increase of cocatalyst loading (above 1:1 ratio) resulted in significant decrease of activity, selectivity and decrease of molar mass. This is due to the displacement of growing polymer chain from active metal center by nucleophilic cocatalyst moieties promoted at higher cocatalyst concentration resulting in increased back-biting of free polymer chains leading to CPC formation. Additionally, PPNCl alone was tested as a catalyst. At identical conditions, only trace amount of cyclic carbonate (TOF<sub>CPC</sub> ≈ 3 h<sup>-1</sup>) was detected in <sup>1</sup>H NMR spectrum of reaction mixture.

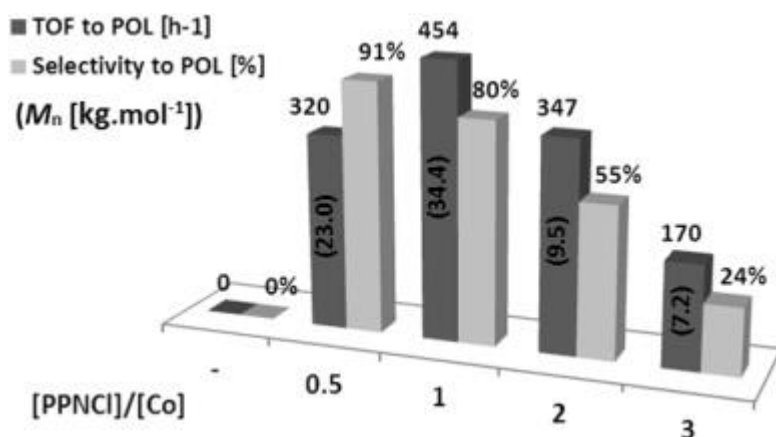


Fig. 3. The effect of **2a**/PPNCl loading to *rac*PO/CO<sub>2</sub> copolymerization at 1 MPa and 50 °C ([PO]/[Co] = 2000:1,  $t_p$  = 2 h).

Using reaction conditions optimized for **2a**/PPNCl system (50 °C, 1 MPa CO<sub>2</sub>, Co/PPNCl = 1:1) a screening of polymerization behavior was performed for the series of salen complexes **2a-c** with phenylene backbone and complexes **3a,b,d** with 3-chlorophenylene backbone bearing different Y nucleophile groups. (Table 3) The results were compared with those published for analogous salen complex **1a** [23]. Complex **2a** with weakest nucleophile – trichloroacetate ( $pK_a$  of conjugated acid 0.65) proved to be the most effective for PO/CO<sub>2</sub> copolymerization to produce PPC with highest activity, molar mass and selectivity up to 80% towards polymer. Complexes bearing stronger nucleophiles, such as **2c** with pentafluorobenzoate ( $pK_a$  = 1.60) and **2b** with 2,4-dinitrophenolate ( $pK_a$  = 4.11) exhibit lower activity, molar mass and also selectivity was decreased to 60%. The decrease of catalyst activity with increase of Y nucleophilicity is caused by the fact that the stronger nucleophile dissociates from metal center more slowly and thus the coordination and subsequent epoxide activation is slower. Similarly, higher affinity of more nucleophilic Y group to metal center leads to higher concentration of uncoordinated polymer chains which undergo the back-biting reaction to CPC which leads to decreased selectivity.

Table 3. Copolymerization of *rac*PO/CO<sub>2</sub> catalyzed with salphen Co complexes **2a–c** and **3a–d** compared with chiral (R,R') salen Co complex (**1a**).

Exp.	Catalyst	Y <sub>w</sub> POL <sup>a</sup> (%)	TOF <sub>POL</sub> <sup>b</sup> (h <sup>-1</sup> )	TOF <sub>CPC</sub> <sup>c</sup> (h <sup>-1</sup> )	M <sub>n</sub> <sup>d,e</sup> (MALLS) (kg mol <sup>-1</sup> )	Đ <sup>d,e</sup>	Selectivity <sup>f</sup> (%) PPC)	HT linkage <sup>g</sup> (%)
Ref [23]	<b>1a</b> <sup>h</sup>	–	568	–	30.9 <sup>i</sup>	1.20 <sup>i</sup>	99	96
6	<b>2</b>	0	0	243	–	–	0	–
2	<b>2a</b>	42.9	456	110	34.4(48 + 25)	1.16	81	92
7	<b>2b</b>	38.0	391	251	21.3(40 + 21)	1.30	61	–
8	<b>2c</b>	36.7	374	228	25.0(41 + 21)	1.28	62	–
9	<b>3a</b>	37.7	386	72	29.4(43 + 23)	1.13	84	95
10	<b>3b</b>	33.2	340	87	14.8(23 + 11)	1.10	80	–
11	<b>3d</b>	12.5	124	184	10.3(10 + 9)	1.05	40	–

Polymerizations run in neat epoxide, [PO]/[Co]/[PPNCI] = 2000:1:1; V<sub>PO</sub> = 1.5–2 mL; T = 50 °C, t<sub>p</sub> = 2 h, p<sub>CO<sub>2</sub></sub> = 1 MPa, Carbonate linkage of all polymers were >99% as determined by <sup>1</sup>HNMR spectroscopy. a Based on isolated polymer yield. b Turnover frequency to polycarbonate. c Turnover frequency to cyclic carbonate; (For details see experimental part). d Determined by SEC-MALLS in THF. e All polymers exhibit bimodal distributions (values in brackets correspond to M<sub>p</sub>). f Selectivity to PPC over cyclic carbonate. g Head-to-tail linkage determined by <sup>13</sup>C NMR spectroscopy. h Ref. [23]: Chiral (R,R')SalenCo-OOCCl<sub>3</sub> complex (Fig. 1), T = 25 °C, t<sub>p</sub> = 1.5 h, p<sub>CO<sub>2</sub></sub> = 1.5 MPa. i Literature data, M<sub>n</sub> and Đ determined by SEC with PS standard calibration in THF.

The substitution of phenylene backbone by Cl atom was further investigated as analogous Cr complex was found to be highly active in similar catalytic ROP of β-butyrolactone [44]. However, in case of CO<sub>2</sub>/PO copolymerization, the activity of chloro substituted Co complexes **3a** and **3b** was lower compared to unsubstituted derivatives **2a** and **2b** (Table 3, runs 9 and 10 vs. 2 and 7). This can be explained by increased Lewis acidity of Co metal center in **3a** and **3b** which lowers the activity of salphen complexes due to the stronger interaction of nucleophile and metal which slows down PO coordination and its attack by nucleophile in initiation and propagation step. As expected, complex **3d** combining chloro substitution on phenylene backbone and the strongest Y nucleophile (acetate group, pK<sub>a</sub> = 4.76) displayed the lowest activity and selectivity in CO<sub>2</sub>/PO copolymerization.

Investigation of temperature dependence of catalytic behavior of complexes shows that **2a** continuously increases its activity up to 75 °C upon while the selectivity simultaneously decreases. Complex **3a** reaches the maximum activity and selectivity at 50 °C (Fig. 4). This shows the importance of optimization of reaction conditions for each of the catalyst to achieve its best catalytic performance. In addition, asymmetric salphen complex **3a** exhibited slightly higher regioselectivity (expressed as head-to-tail linkage %) compared to corresponding symmetric complex **2a** (Table 3, exp. 2 vs. 9).

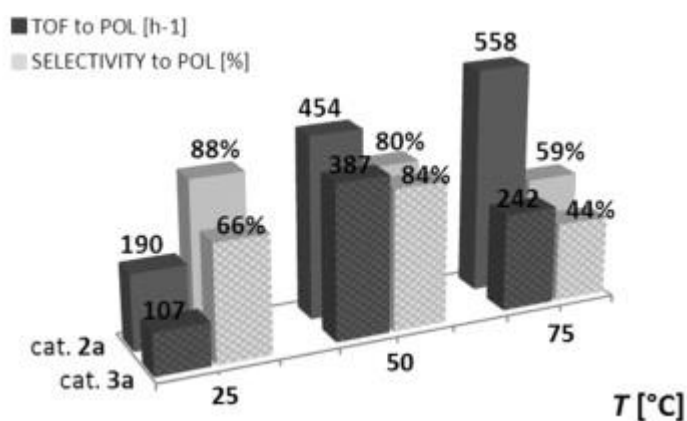


Fig. 4. The effect of catalyst and temperature to overall activity and selectivity of *rac*PO/CO<sub>2</sub> copolymerization catalyzed by salphen Co complexes **2a**/PPNCl and **3a**/PPNCl at 1 MPa ([M]/[CAT] = 2000:1).

All prepared polypropylene carbonates displayed bimodal molar mass distribution as already observed for other salen complexes earlier [42], [50].  $M_n$  value of the higher-molar-mass peak was twice as large as that of the lower-molar-mass one in all prepared polycarbonates. This was previously described and explained due to the presence of contaminant water, which works as a bifunctional initiating group to give a telechelic polymers [42], [47], [50]. This indicate, that copolymerization can be initiated by several different active species such as axial Y group of catalyst and a chlorine anion which is a part of PPNCl cocatalyst or also by contaminant water.

To clear up the mechanism of activation, the MALDI-TOF analysis of prepared polycarbonates was used to determine end-groups of final polymer (Fig. 5). Probably due to poor ionization of polycarbonate samples and their fragmentation, only low molar mass fractions of polymers up to 3 kg.mol<sup>-1</sup> were detected. Obtained spectra for PPC prepared by **3b**/PPNCl revealed presence of DNP ( $\alpha$  end group) and catalyst adduct ( $\omega$  end group). Catalyst  $\omega$  end group can be attached either to ether or carbonate oxygen (Fig. 5).

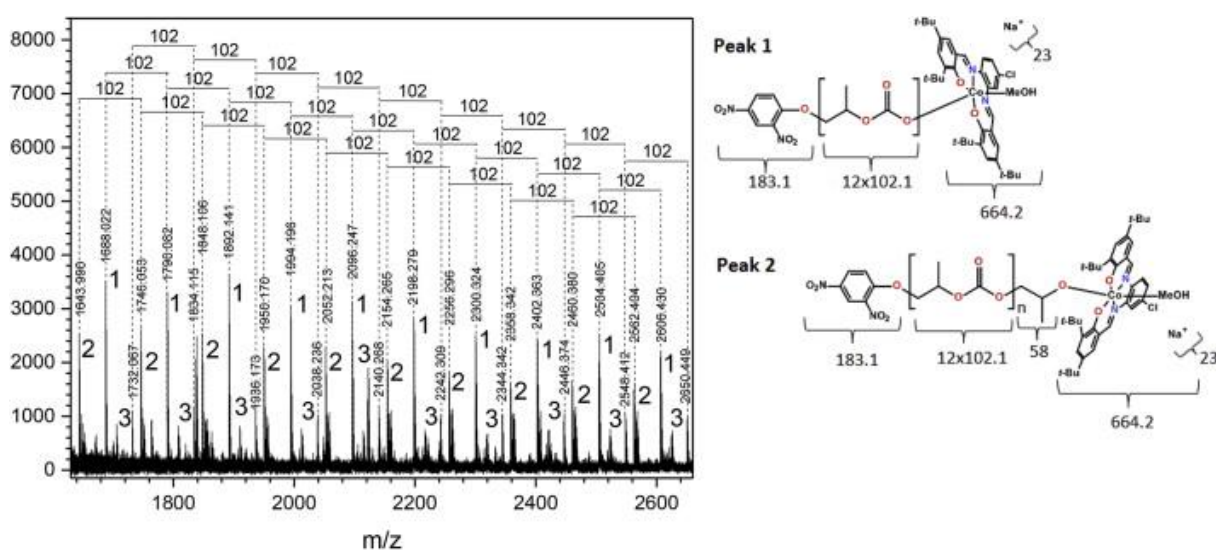


Fig. 5. MALDI-TOF spectrum of PPC prepared by **3b**/PPNCl (exp. 10).

For peak 1 we detected molar mass corresponding to initiation by DNP<sup>-</sup> and termination by adduct **3**-MeOH attached to carbonate oxygen (see Fig. 5):  $M_{\text{Peak1}} (2096.2) = M_{\text{DNP}} (183.1) + M_{\text{Na}^+} (23) + 12x M_{\text{C}_4\text{H}_6\text{O}_3} (1225.1) + M_{\text{3-MeOH}} (664.2) = 2095.4 \text{ g mol}^{-1}$ . Peak 2 correspond to initiation by DNP<sup>-</sup> and termination by adduct **3**-MeOH attached to ether oxygen:  $M_{\text{Peak2}} (2052.2) = M_{\text{DNP}} (183.1) + M_{\text{Na}^+} (23) + 11x M_{\text{C}_4\text{H}_6\text{O}_3} (1123) + M_{\text{C}_3\text{H}_6\text{O}} (58) + M_{\text{3-MeOH}} (664.2) = 2051.3 \text{ g mol}^{-1}$ . Peak 3 was attributed to structure where DNP<sup>-</sup> and **3**-H<sub>2</sub>O adduct attached to ether oxygen are presented as end groups of polycarbonate:  $M_{\text{Peak3}} (2038.2) = M_{\text{DNP}} (183.1) + M_{\text{Na}^+} (23) + 11x M_{\text{C}_4\text{H}_6\text{O}_3} (1123) + M_{\text{C}_3\text{H}_6\text{O}} (58) + M_{\text{3-H}_2\text{O}} (650.2) = 2037.3 \text{ g mol}^{-1}$

For comparison reasons we also used (salphen)Co(II) complex **2** for *rac*-PO/CO<sub>2</sub> copolymerization (Table 3, exp. 6). In combination with PPNCl the complex **2** was able to catalyze the cyclization reaction to CPC at much higher TOF (243 h<sup>-1</sup>) than PPNCl alone (3 h<sup>-1</sup>).

### 2.3. Alternating copolymerization of cyclohexene oxide with CO<sub>2</sub> in presence of (salphen)CoY complexes

Salphen Co (III) complexes were further tested for copolymerization of CHO with CO<sub>2</sub> which leads to polycarbonates with higher  $T_g$  (Table 4). Copolymerization conditions were optimized with salphen complex **3d**, founding [Co]/[PPNCl] = 1:1 at [CHO]/[Co] = 1000-2000:1, 1 MPa and 75 °C affording PCHC with molar mass around 20 kg mol<sup>-1</sup> and TOF 260–290 h<sup>-1</sup> (Table 4, exp. 13, 14). A 100% selectivity to copolymer with no production of cyclohexene carbonate byproduct during CHO/CO<sub>2</sub> copolymerization is attributed to high (86 kJ mol<sup>-1</sup>) difference of activation barriers for cyclic carbonate formation compared to the formation of PCHC [29]. Decrease of reaction temperature from 75 °C to 50 °C or decrease of pressure from 1 MPa to 0.1 MPa resulted in 50% decrease of polycarbonate formed molar mass and 2-5 times polymerization rate reduction (Table 4, exp. 13 vs. 12 and 16).

Table 4. Copolymerization of CHO with CO<sub>2</sub> with salphen Co complex **3d** compared to literature data obtained with Salen complexes **1b** and **1c**.

Exp.	Catalyst	$T$ (°C)	$p$ (MPa)	[CHO]/[Co]/[PPNCl]	$Y_{w \text{ POL}}^a$ (%)	TOF <sub>POL</sub> <sup>b</sup> (h <sup>-1</sup> )	$M_n$ (MALLS) <sup>c,d</sup> (kg mol <sup>-1</sup> )	$\bar{D}^{c,d}$
Ref [23]	<b>1b</b> <sup>e</sup>	40	1.5	1000:1:1	–	298	18.3 <sup>g</sup>	1.20 <sup>g</sup>
Ref [46]	<b>1c</b> <sup>f</sup>	70	0.7	1000:1:1	44	440	11.9 <sup>g</sup>	1.23 <sup>g</sup>
12	<b>3d</b>	50	1	1000:1:1	27.8	133	13.8(18 + 10)	1.08
13	<b>3d</b>	75	1	1000:1:1	45.8	263	21.5(30 + 16)	1.12
14	<b>3d</b>	75	1	2000:1:1	29.4	287	23.1(29 + 16)	1.08
15 <sup>h</sup>	<b>3d</b>	75	1	1000:1:0.5	45.3	161	23.8(36 + 19)	1.15
16	<b>3d</b>	75	0.1	1000:1:1	12.9	64	8.9	1.07

Polymerizations run in neat epoxide;  $V_{\text{CHO}} = 1.5\text{--}2 \text{ mL}$ ,  $t_p = 2 \text{ h}$ ; Selectivity to polycarbonate as determined by <sup>1</sup>H NMR spectroscopy was >99% in all cases; All poly(cyclohexene carbonate)s have >99% carbonate linkages as determined by <sup>1</sup>H NMR spectroscopy. a Based on isolated polymer yield. b Turnover frequency to polycarbonate. c Determined by SEC-MALLS in THF. d All polymers exhibit bimodal distributions (values in brackets correspond to  $M_p$ ). e Catalyzed with chiral (R,R')SalenCo-DNP complex (Fig. 1). f Catalyzed with chiral (R,R')Salen Co-OBzF<sub>3</sub> complex (Fig. 1). g Literature data,  $M_n$  and  $\bar{D}$  determined by SEC on PS standards calibration in THF. h  $t_p = 3 \text{ h}$ .

The variation of Y nucleophile (Table 5) has only a little effect to Co complexes activity and molar mass of resulted polycarbonates, except of complex **2a**, which was significantly less active compared to other complexes **2b,c** and **3a-d**. Surprisingly the complexes **2a** and **3a** containing the same nucleophile show considerable different activity which is not possible to ascribe to the ligand substitution by Cl atom in **3a** as the same ligands in **2b** and **3b** have no effect on their activity. All complexes produced PCHC with 100% selectivity to polymer (no formation of cyclic carbonate) and >99% of carbonate linkage at 75 °C and 1 MPa. Number average molar mass values of PCHC prepared by **2b,c** and **3a-d** were in the range of 15–23 kg mol<sup>-1</sup>, again displaying a bimodal molar mass distribution as in the case of polypropylene carbonates described above.

Table 5. Copolymerization of cyclohexene oxide with CO<sub>2</sub> with salphen Co complexes **2a-c** and **3a-d**.

Exp.	Catalyst	Y <sub>w,POL</sub> <sup>a</sup> (%)	TOF <sub>POL</sub> <sup>b</sup> (h <sup>-1</sup> )	M <sub>n</sub> (MALLS) <sup>c,d</sup> (kg mol <sup>-1</sup> )	Đ <sup>c,d</sup>
17	<b>2a</b>	20.6	106	8.7(14 + 7)	1.41
18	<b>2b</b>	46.0	222	20.0(29 + 15)	1.14
19	<b>2c</b>	46.5	236	21.0(30 + 16)	1.22
20	<b>3a</b>	42.4	276	18.4(30 + 15)	1.27
21	<b>3b</b>	45.3	230	17.3(26 + 13)	1.10
13	<b>3d</b>	45.8	263	23.0(29 + 15)	1.09

Polymerizations run in neat epoxide; V<sub>CHO</sub> = 1.5–2 mL, T = 75 °C, t<sub>p</sub> = 2 h, p<sub>CO<sub>2</sub></sub> = 1 MPa [CHO]/[Co]/[PPNCI] = 1000:1:1; In all cases cyclohexene carbonate byproduct is not observed and all poly(cyclohexene carbonate)s have >99% carbonate linkages as determined by <sup>1</sup>H NMR spectroscopy. a Based on isolated polymer yield. b Turnover frequency to polycarbonate. c Determined by SEC-MALLS in THF. d All polymers exhibit bimodal distributions (values in brackets correspond to M<sub>p</sub>).

The M<sub>n</sub> and M<sub>p</sub> values of PCHC prepared with catalytic system **2a**/PPNCI increased linearly in proportion to conversion in the range of 0–30% (Fig. 6) while dispersity remained relatively low (Đ = 1.1–1.4) indicating controlled manner of these catalytic polymerizations [51].

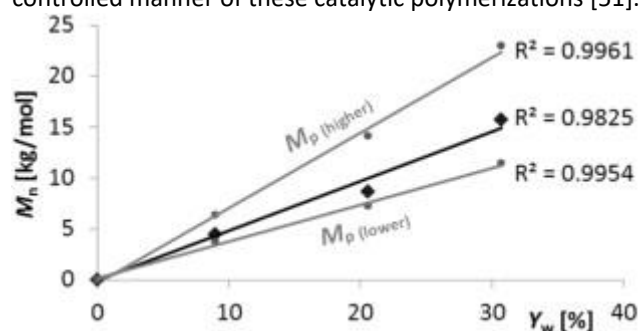


Fig. 6. Linear increase of PCHC molar mass with conversion (catalytic system **2a**/PPNCI, [PO]/[Co]/[PPNCI] = 1000:1:1, t<sub>p</sub> = 0.5, 2 and 4 h, T = 75 °C, p = 1 MPa).

MALDI-TOF analysis of synthesized PCHC prepared by **2a**/PPNCI (Fig. 7) confirmed the presence of OOCCL<sub>3</sub><sup>-</sup> and Cl<sup>-</sup> anions (α end groups) and PPN<sup>+</sup> and (Salphen)Co.MeOH (ω end groups) respectively. In contrast to PPC polymer, (Salphen)Co<sup>+</sup> and PPN<sup>+</sup> ω end groups are attached solely to carbonate oxygen showing that the last monomer unit comes from CO<sub>2</sub> insertion, probably due to higher steric hindrance of CHO units compared to PO.

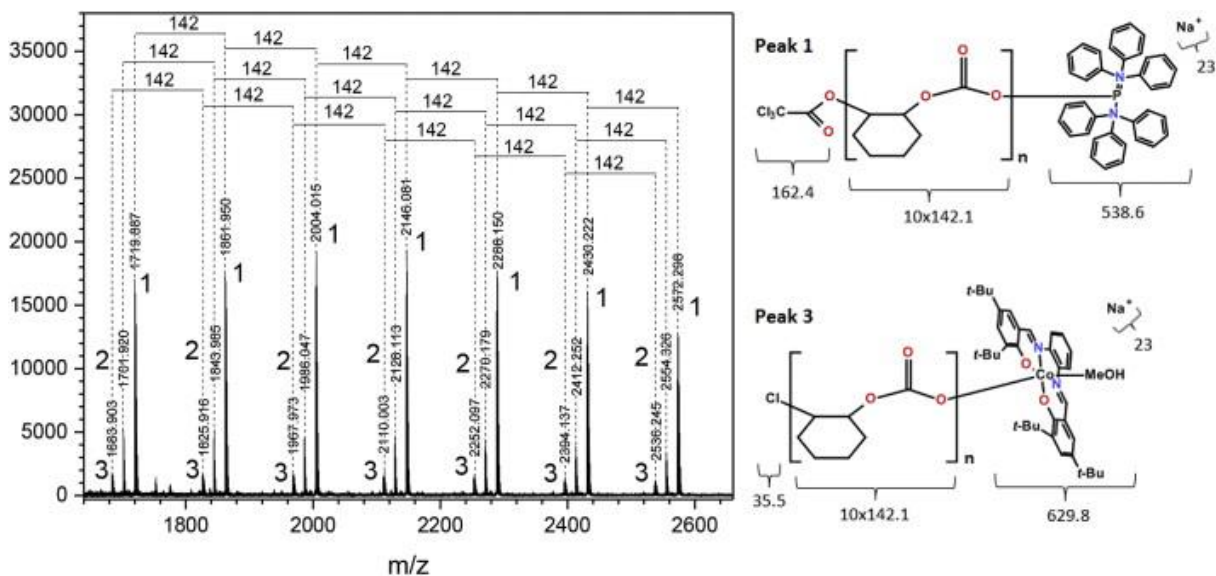


Fig. 7. MALDI-TOF spectrum of PCHC prepared by **2a**/PPNCl (exp. 17).

Peak 1 was attributed to polycarbonate with  $\text{OOCCH}_2\text{Cl}$  and  $\text{PPN}^+$  end groups:  $M_{\text{Peak1}} (2146.1) = M_{\text{OOCCH}_2\text{Cl}} (162.4) + M_{\text{Na}^+} (23) + 10 \times M_{\text{C}_7\text{H}_{10}\text{O}_3} (142.1) + M_{\text{PPN}^+} (538.6) = 2145.5 \text{ g mol}^{-1}$ .

Peak 3 was attributed to polycarbonate with  $\text{Cl}^-$  ( $\alpha$  end groups) and 2-MeOH adduct ( $\omega$  end group):  $M_{\text{Peak3}} (2110.0) = M_{\text{Cl}^-} (35.5) + M_{\text{Na}^+} (23) + 10 \times M_{\text{C}_7\text{H}_{10}\text{O}_3} (142.1) + M_{2\text{-MeOH}} (629.8) = 2109.8 \text{ g mol}^{-1}$  (Fig. 7).

Peak 2 could be composed of same  $\alpha$  and  $\omega$  end groups as peak 3 with one more water molecule attached to Co metal:  $M_{\text{Peak2}} (2128.1) = M_{\text{Cl}^-} (35.5) + M_{\text{Na}^+} (23) + 10 \times M_{\text{C}_7\text{H}_{10}\text{O}_3} (142.1) + M_{2\text{-MeOH}} (629.8) + M_{\text{H}_2\text{O}} (18) = 2127.8 \text{ g mol}^{-1}$ .

MALDI TOF spectra of PCHC shows that both nucleophiles ( $\text{OOCCH}_2\text{Cl}$ ,  $\text{Cl}^-$ ) initiate the growth of polycarbonate chain and both counteranions can be connected as the  $\omega$  end group.

### 3. Conclusions

Herein, we reported a series of novel salphen Co(III)-Y complexes, which were effective for both PO/ $\text{CO}_2$  and CHO/ $\text{CO}_2$  copolymerization leading to polycarbonates (>99% carbonate linkage) with molar mass 15–30  $\text{kg mol}^{-1}$  and narrow dispersity. Substitution of phenylene framework of salphen ligand by chlorine atom led to decrease of activity in PO/ $\text{CO}_2$  copolymerization. Variation of Y counteranions on PO/ $\text{CO}_2$  copolymerization showed significant differences in activity, selectivity and molar mass, the best results were obtained with complexes bearing the weakest nucleophile trichloroacetate. PO/ $\text{CO}_2$  copolymerization catalyzed by salphen Co complexes was accompanied by formation of cyclic carbonate (20–60%). Activity and selectivity of all salphen Co (III) complexes in CHO/ $\text{CO}_2$  copolymerization was almost independent on ligand structure and counteranion. No cyclic carbonate was formed in CHO/ $\text{CO}_2$  copolymerization even at low  $\text{CO}_2$  pressures.

### 4. Experimental part

#### 4.1. General information

All manipulation involving water or air sensitive compounds were carried out using standard Schlenk techniques under dry nitrogen. Propylene oxide (Aldrich) and cyclohexene oxide (Aldrich) were dried under  $\text{CaH}_2$  and distilled under vacuum or  $\text{N}_2$  atmosphere. PPNCl (ABCR) was purified by precipitation of its dry dichloromethane solution in dry diethylether. 1,2-phenylenediamine, 4-chloro-1,2-phenylenediamine, 3,5-ditert-butyl-2-hydroxybenzaldehyde, cobalt(II)acetate tetrahydrate (all Aldrich), pentafluorobenzoic acid and trichloroacetic acid (both Alfa Aesar) were used as received. 2,4-dinitrophenol (Aldrich, stabilized with 15%  $\text{H}_2\text{O}$ ) was dried under high vacuum to remove water prior to use. Dichloromethane, diethylether and hexane were dried over  $\text{CaH}_2$  and distilled under  $\text{N}_2$  atmosphere. Water content of monomers and solvents was determined by Karl Fischer titration. Nitrogen (5.0, SIAD) was purified by passing through deoxygenating and drying columns.  $\text{CO}_2$  (4.8, SIAD) was used without further purification.

#### 4.2. Synthesis of complexes

N,N'-Bis(3,5-di-tert-butylsalicylidene)-1,2-phenylenediamine (**L2**) and N,N'-Bis(3,5-di-tert-butylsalicylidene)-4-chloro-1,2-phenylenediamine (**L3**) were synthesized according to literature [44].

##### 4.2.1. (N,N'-Bis(3,5-di-tert-butylsalicylidene)-1,2-phenylenediamine)Cobalt(II) (**2**)

It was synthesized according to modified literature procedure [52]. Degassed ethanol (150 mL) was added to a flask charged with ligand (**L2**) (3.5 mmol). Suspension was heated to 50 °C until complete ligand dissolution. Then cobalt(II) acetate tetrahydrate (0.7 g, 2.9 mmol) was dissolved in 30 mL of degassed EtOH and immediately added dropwise to solution of **L2**. The flask was heated to 80 °C for 30 min and then slowly cooled to room temperature. Final suspension was concentrated to cca 70 mL, filtered under nitrogen atmosphere and washed with cold (-20 °C) dried methanol. The dark red/brown powder was recrystallized by dissolving it in dry methylene chloride (30 mL) and layered with dry hexane (700 mL). Solution was let few days to recrystallize in the fridge and then filtered under nitrogen atmosphere and dried 24 h under high vacuum.  $Y_w = 80\%$ .

MS-ESI<sup>+</sup> ( $m/z$ ,  $M^+$ ) = 597.2888; Calcd. For:  $[\text{C}_{36}\text{H}_{46}\text{N}_2\text{O}_2\text{Co}]^+$ : 597.2886.

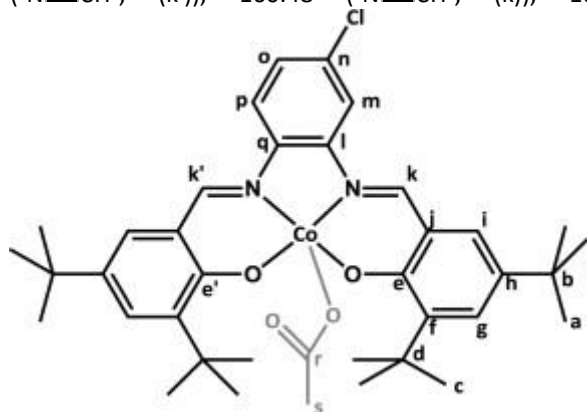
IR (ATR,  $\text{cm}^{-1}$ ): 2954, 2902, 2866, 1613, 1574, 1543, 1519, 1489, 1463, 1424, 1386, 1355, 1323, 1249, 1198, 1178, 1161, 1131, 930, 918, 785, 740, 638.

##### 4.2.2. (N,N'-Bis(3,5-di-tert-butylsalicylidene)-4-chloro-1,2-phenylenediamine)Cobalt(II) (**3**)

It was synthesized as **2**.  $Y_w = 90\%$ .

$^1\text{H}$  NMR (DMSO- $d_6$ , 500 MHz):  $\delta$  1.33 (18H,  $-\text{CH}_3$  (**b**)), 1.69 (s, 18H,  $-\text{CCH}_3$  (**a**)), 7.39 (2H,  $=\text{CH}-$  (**g**)); 7.47 (2H, ArH (**i**)), 7.50 (1H, ArH (**o**)), 8.47 (1H, ArH (**p**)), 8.61 (1H, ArH (**m**)), 8.71 (1H,  $-\text{N}=\text{CH}-$  (**k'**)), 8.77 (1H,  $-\text{N}=\text{CH}-$  (**k**));

$^{13}\text{H}$  NMR (DMSO- $d_6$ , 500 MHz): 30.09 (-CH $_3$  (a)), 31.24 (-CH $_3$  (c)), 33.61 (-C(CH $_3$ ) $_3$  (d)), 35.84 (-C(CH $_3$ ) $_3$  (b)), 116.10 (=CH- Ar, (m)), 116.91 (=CH- Ar, (p)), 117.76 (=C- Ar, (j)), 125.90 (=C- Ar, (o)), 129.13 (=CH- Ar, (i)), 129.57 (=CH- Ar, (g)), 131.09 (=CCl-Ar (n)), 134.59 (=C-Ar (f)), 141.63 (=C-Ar (h)), 145.31(=C-Ar, (q)), 147.35(=C-Ar, (l)), 159.97 (-N=CH-, (k')), 160.48 (-N=CH-, (k)), 166.06 (=C-O Ar (e')), 166.46 (=C-O Ar (e)).



MS-ESI $^+$  ( $m/z$ ,  $M^+$ ) = 631.2499; Calcd. For: [C $_{36}$ H $_{45}$ N $_2$ O $_2$ ClCo] $^+$ : 631.2496.

IR (ATR,  $\text{cm}^{-1}$ ): 2953, 2904, 2867, 1607, 1574, 1543, 1519, 1484, 1463, 1425, 1387, 1358, 1334, 1261, 1197, 1170, 1161, 1131, 1122, 1090, 935, 910, 785, 806, 748.

Complexes **2a–c** and **3a,b,d** were synthesized according to the literature method [23], [52].

#### 4.2.3. Synthesis of complex 2a

To a stirred mixture of **2** (0.6040 g, 1 mmol) in dry CH $_2$ Cl $_2$  (20 mL) was added trichloroacetic acid (0.1840 g, 1 mmol, 1 equiv.) in CH $_2$ Cl $_2$  (15 mL). The solution was stirred under dry oxygen atmosphere at room temperature for 90 min. The solvents were removed in vacuo and dark red/brown solid was dried under high vacuum. Crude product was washed 3x with 20 mL of dry hexane and dried 24 h under high vacuum.  $Y_w$  = 78%. (Complex is mixture of complex with one Y $^-$  group and complex with one Y $^-$  group and coordinated YH molecule).

MS-ESI $^{+/-}$  ( $m/z$ ,  $M^+$ ) = 597.2883; Calcd. For: [C $_{36}$ H $_{46}$ N $_2$ O $_2$ Co] $^+$ : 597.2886.

IR (ATR,  $\text{cm}^{-1}$ ): 2959, 2905, 2868, **1718**, **1704** (C=O vibrations of CCl $_3$ COO $^-$ ), 1612, 1578, 1546, 1519, 1486, 1461, 1418, 1387, 1358, 1330, **1288** (C–O vibration of CCl $_3$ COO $^-$ ), 1199, 1182, 1167, 1133, 1110, **883** (C–Cl vibration of CCl $_3$ COO $^-$ ), 753, 676.

EA calculated for [C $_{36}$ H $_{46}$ N $_2$ O $_2$ Co (C $_2$ Cl $_3$ O $_2$ ) $_{1.75}$ ] (%): C 53.80; H 7.76; N 3.18; Found: C 53.93; H 5.37; N 3.28.

#### 4.2.4. Synthesis of complex 2b

It was synthesized as a similar procedure of the complex **2a**. Crude product was washed 3x with 20 mL of mixture hexane/ethyl acetate (dry) (50/50) and dried 24 h under high vacuum.  $Y_w$  = 61%.

MS-ESI $^{+/-}$  ( $m/z$ ,  $M^+$ ) = 597.2888; Calcd. For: [C $_{36}$ H $_{46}$ N $_2$ O $_2$ Co] $^+$ : 597.2886; ( $m/z$ ,  $M^-$ ): 183.0041; Calcd. for [C $_6$ H $_3$ N $_2$ O $_5$ ] $^-$ ; 183.0036.

IR (ATR,  $\text{cm}^{-1}$ ): 2952, 2904, 2867, **1610**, **1576** (N=O vibration of DNP), 1519, 1519, 1489, 1462, 1428, 1389, 1358, **1319** (N=O vibration of DNP), 1267, 1248, 1197, 1174, 1130, 936, 919, 833, 784, 743.

$^1\text{H}$  NMR (DMSO- $d_6$ , 500 MHz):  $\delta$  1.35 (18H,  $-\text{CH}_3$  (b)), 1.78 (s, 18H,  $-\text{CCH}_3$  (a)), 6.42 (1H, ArH (DNP)), 7.56 (4H, ArH (i,g)), 7.65 (2H, ArH (n)), 7.84 (1H, ArH (DNP)), 8.63 (3H, ArH (m + DNP)), 8.93 (2H,  $-\text{N}=\text{CH}$ -(k)).

EA calculated for  $[\text{C}_{36}\text{H}_{46}\text{N}_2\text{O}_2\text{Co} (\text{C}_6\text{N}_2\text{O}_5)_{0.85}]$  (%): C 65.53; H 6.50; N 6.88; Found: C 65.53; H 6.76; N 6.28.

#### 4.2.5. Synthesis of complex 2c

It was synthesized by a similar procedure as the complex **2a**.  $Y_w = 53\%$ . Crystals suitable for X-ray analysis were prepared by layering technique (solvent diffusion). Cca 10 mg of complex **2c** was placed into dry clean NMR tube under nitrogen and dissolved in (cca 0.3 mL of dry  $\text{CH}_2\text{Cl}_2$ ). Solution was then layered by slow dribbling of dry hexane (2.5–3 mL). The NMR tube was then carefully placed in a quiet place for 2–3 weeks until dark red block-shaped crystals occurred.

MS-ESI $^+$  ( $m/z$ ,  $M^+$ ) = 597.2893; Calcd. For:  $[\text{C}_{36}\text{H}_{46}\text{N}_2\text{O}_2\text{Co}]^+$ : 597.2886; ( $m/z$ ,  $M^-$ ): 166.9932; Calcd. for  $[\text{C}_6\text{F}_5]$ , 166.9926; and; ( $m/z$ ,  $M^-$ ): 210.9817; Calcd. for  $[\text{C}_7\text{F}_5\text{O}_2]$ , 210.9824.

IR (ATR,  $\text{cm}^{-1}$ ): 2955, 2906, 2869, 1734, **1666**, **1651** ( $\text{C}=\text{O}$  vibrations of  $\text{OBzF}_5^-$ ), 1612, 1592, 1581, 1520, 1485, 1463, 1423, **1387** ( $\text{C}-\text{F}$  vibration of  $\text{OBzF}_5^-$ ), 1356, 1331, 1274, 1241, 1197, 1170, 1133, 1112, **995** ( $\text{C}-\text{F}$  vibration of  $\text{OBzF}_5^-$ ), 761, 749.

$^1\text{H}$  NMR (DMSO- $d_6$ , 500 MHz):  $\delta$  1.35 (18H,  $-\text{CH}_3$  (b)), 1.78 (s, 18H,  $-\text{CCH}_3$  (a)), 7.40 (2H,  $=\text{CH}$ - (g)); 7.46 (2H, ArH (i)), 7.56 (2H, ArH (m)), 8.64 (2H, ArH (m)), 8.95 (2H,  $-\text{N}=\text{CH}$ -(k))

$^{19}\text{F}$  NMR (500 MHz, DMSO- $d_6$ ): -138.96, -143.73, -154.57, -157.57, -162.28.

EA calculated for  $[\text{C}_{36}\text{H}_{46}\text{N}_2\text{O}_2\text{Co} (\text{C}_7\text{F}_5\text{O}_2)_{1.75}]$ (%): C 59.93; H 4.79; N 2.90; Found: C 60.00; H 5.32; N 2.89.

#### 4.2.6. Synthesis of complex 3a

It was synthesized by a similar procedure as the complex **2a** using precursor **3**.  $Y_w = 52\%$ .

MS-ESI $^{+/-}$  ( $m/z$ ,  $M^+$ ) = 631.2497; Calcd. For:  $[\text{C}_{36}\text{H}_{45}\text{N}_2\text{O}_2\text{ClCo}]^+$ : 631.2496.

IR (ATR,  $\text{cm}^{-1}$ ): 2958, 2907, 2869, **1761**, **1697** ( $\text{C}=\text{O}$  vibrations of  $\text{CCl}_3\text{COO}^-$ ), 1603, 1580, 1522, 1483, 1418, 1383, 1359, 1307, **1254** ( $\text{C}-\text{O}$  vibration of  $\text{CCl}_3\text{COO}^-$ ), 1197, 1167, 1126, 1092, 937, **836** ( $\text{C}-\text{Cl}$  vibration of  $\text{CCl}_3\text{COO}^-$ ), 755, 683.

EA calculated for  $[\text{C}_{36}\text{H}_{45}\text{N}_2\text{O}_2\text{ClCo} (\text{C}_2\text{Cl}_3\text{O}_2)_{2.05}]$  (%): C 49.91; H 4.70; N 2.90; Found: C 50.01; H 5.13; N 2.81.

#### 4.2.7. Synthesis of complex 3b

It was synthesized by a similar procedure as the complex **3a**. Crude product was washed 3x with 20 mL of mixture hexane/ethyl acetate (dry) (50/50) and dried 24 h under high vacuum.  $Y_w = 65\%$ .

MS-ESI $^{+/-}$  ( $m/z$ ,  $M^+$ ) = 631.2499; Calcd. For:  $[\text{C}_{36}\text{H}_{45}\text{N}_2\text{O}_2\text{ClCo}]^+$ : 631.2496; ( $m/z$ ,  $M^-$ ): 183.0055; Calcd. for  $[\text{C}_6\text{H}_3\text{N}_2\text{O}_5]$ : 183.0047.

IR (ATR,  $\text{cm}^{-1}$ ): 2952, 2904, 2867, 1600, 1573, 1545, 1519, 1483, 1462, 1424, 1389, 1357, **1327** ( $\text{N}=\text{O}$  vibration of DNP), 1262, 1196, 1174, 1131, 1122, 934, 912, 835, 783, 744.

$^1\text{H}$  NMR (DMSO- $d_6$ , 500 MHz):  $\delta$  1.35 (18H,  $-\text{CH}_3$  (c)), 1.78 (s, 18H,  $-\text{CCH}_3$  (a)), 6.99 (1H, ArH (DNP)), 7.40 (2H,  $=\text{CH}-$  (g)); 7.51 (2H, ArH (i)), 7.56 (1H, ArH (o)), 8.20 (1H, ArH (DNP)), 8.57 (1H, ArH (p)), 8.70 (1H, ArH (m + DNP)), 8.93 (1H,  $-\text{N}=\text{CH}-$  (k)), 8.97 (1H,  $-\text{N}=\text{CH}-$ (k')).

EA calculated for  $[\text{C}_{36}\text{H}_{45}\text{N}_2\text{O}_2\text{ClCo}(\text{C}_6\text{N}_2\text{O}_5)_{1.80}]$  (%): C 58.45; H 5.28; N 8.16; Found: C 58.40; H 5.75; N 6.37.

#### 4.2.8. Synthesis of complex 3d

It was synthesized according to the literature [52].  $Y_w = 99\%$ .

MS-ESI $^+$  ( $m/z$ ,  $M^+$ ) = 631.2484; Calcd. For:  $[\text{C}_{36}\text{H}_{45}\text{N}_2\text{O}_2\text{ClCo}]^+$ : 631.2496.

IR (ATR,  $\text{cm}^{-1}$ ): 2950, 2904, 2867, 1603, 1572, 1543, 1519, 1484, 1462, 1424, 1357, 1263, 1197, 1173, 1159, 1121, 934.

EA calculated for  $[\text{C}_{36}\text{H}_{45}\text{N}_2\text{O}_2\text{ClCo}(\text{C}_2\text{H}_3\text{O}_2)_{1.30}]$  (%): C 65.40; H 6.95; N 3.95; Found: C 65.43; H 7.25; N 4.18.

### 4.3. Copolymerization of PO and CHO with $\text{CO}_2$

A 100 mL Fischer-Porter bottle was heated to 100 °C in an oven for 60 min. Immediately after removing from an oven, the Fischer-Porter bottle was screwed to the pressure pipe and purified by few vacuum/ $\text{N}_2$  cycles. The reactor was then shortly opened to air. Solid catalyst and cocatalyst were introduced rapidly and bottle was closed and purified by vacuum/ $\text{CO}_2$  cycles. The epoxide (1.5–2 mL) was then introduced via syringe through the ball valve against flow of  $\text{CO}_2$ . Fischer Porter bottle was pressurized to 1 MPa and heated to desired temperature using an oil bath. After desired polymerization time, the reaction mixture was cooled to  $-78$  °C, excess of pressure was carefully vented of and polymerization vessel was disassembled. A small aliquot of reaction mixture was removed from the reactor for  $^1\text{H}$  NMR analysis. A viscous reaction mixture was then dissolved in small amount of  $\text{CH}_2\text{Cl}_2$  and precipitated into excess of MeOH. Final polymer was separated by filtration and dried 24 h under high vacuum at 60 °C.

### 4.4. Analysis

$^1\text{H}$  and  $^{13}\text{C}$  NMR spectra of ligands, complexes, reaction mixtures and polymers were recorded on Bruker 500 Avance III using  $\text{CDCl}_3$  or DMSO- $d_6$  at room temperature. Elemental analysis of complexes was measured on EI III instrument, from Elementar Vario. The resulting values are average values of two analyses. Mass spectra were recorded on spectrometer Orbitrap Velos (Thermo, USA). Samples were dissolved  $\text{CH}_2\text{Cl}_2$  and then transferred into MeOH. The isocratic methanol was used as mobile phase. FT-IR spectra were recorded on spectrometer Nicolet 6700 by ATR technique. Crystallographic data for complex **2c** were collected on Nonius KappaCCD diffractometer equipped with Bruker APEX-II CCD detector by monochromatized MoK  $\alpha$  radiation ( $\lambda = 0.71073$  Å) at the temperature of 150 K.

MALDI-TOF MS mass spectra were acquired with an UltrafleXtreme (Bruker Daltonics, Bremen, Germany) in the positive ion reflectron mode. The spectra were the sum of 25,000 shots with a DPSS, Nd: YAG laser (355 nm, 1000 Hz). Delayed extraction and external calibration was used. The samples were prepared by the dried droplet method: solutions of polycarbonate sample (10 mg mL<sup>-1</sup>), DCTB (trans-2-[3-(4-t-butyl-phenyl)-2-methyl-2-propenylidene]malonitrile; 10 mg mL<sup>-1</sup>) as a matrix and sodium trifluoroacetate (CF<sub>3</sub>COONa; 10 mg mL<sup>-1</sup>) as a cationization agent in DMF were mixed in the volume ratio 4:20:1. 1 mL of the mixture was deposited on the ground-steel target plate. Drop was dried at ambient atmosphere.

Absolute molar masses were determined using a chromatograph Waters Breeze with RI detector operating at wavelength 880 nm and with MALLS detector miniDawn TREOS (Wyatt). Detector operated at wavelength of 658 nm. Both methods (absolute and PS calibration) were used for determination of molar mass and subsequently correlated. Absolute molar masses of polypropylene carbonates were determined using dn/dc increment 0.050 ± 0.003 mL g<sup>-1</sup>. Analyzed PPC's were on average 12% superior compared to PS calibration values (Figure S1a in Supp. information). Absolute molar masses of analyzed PCHC were calculated with dn/dc increment 0.087 ± 0.002 mL g<sup>-1</sup> and they are by 29% higher compared to *M<sub>n</sub>*'s obtained from PS calibration method (Figure S1b in Supp. information).

## Acknowledgement

This work was supported from specific university research (MSMT No 20/2015). The authors would like to thank to Zuzana Kálalová (Institute of macromolecular chemistry AS CR) for MALDI spectra measurements and Ivana Bartošová (Central laboratories, ICT Prague) for measured NMR spectra. Authors would like to acknowledge suggestions of the reviewers which led to significant improvement of the paper.

## References

- [1] T. Sakakura, K. Kohno Chem Commun (2009), pp. 1312-1330
- [2] M. Aresta (Ed.), Carbon dioxide as chemical feedstock, Wiley-VCH Verlag GmbH & Co. KGaA (2010)
- [3] S. Inoue, H. Koinuma, T. Tsuruta J Polym Sci Part B, 7 (1969), pp. 287-292
- [4] S. Klaus, M.W. Lehenmeier, C.E. Anderson, B. Rieger Coord Chem Rev, 255 (2011), pp. 1460-1479
- [5] M.R. Kember, A. Buchard, C.K. Williams Chem Commun, 47 (2011), pp. 141-163
- [6] M. Cheng, D.R. Moore, J.J. Reczek, B.M. Chamberlain, E.B. Lobkovsky, G.W. Coates J Am Chem Soc, 123 (2001), pp. 8738-8749
- [7] B.Y. Lee, H.Y. Kwon, S.Y. Lee, S.J. Na, Han S-i, H. Yun, et al. J Am Chem Soc, 127 (2005), pp. 3031-3037
- [8] D.R. Moore, M. Cheng, E.B. Lobkovsky, G.W. Coates J Am Chem Soc, 125 (2003), pp. 11911-11924
- [9] R.L. Paddock, S.T. Nguyen Macromolecules, 38 (2005), pp. 6251-6253
- [10] Z. Qin, C.M. Thomas, S. Lee, G.W. Coates Angew Chem Int Ed, 42 (2003), pp. 5484-5487
- [11] R. Eberhardt, M. Allmendinger, B. Rieger Macromol Rapid Commun, 24 (2003), pp. 194-196
- [12] D.J. Darensbourg, R.M. Mackiewicz, J.L. Rodgers, C.C. Fang, D.R. Billodeaux, J.H. Reibenspies Inorg Chem, 43 (2004), pp. 6024-6034
- [13] D.J. Darensbourg, R.M. Mackiewicz J Am Chem Soc, 127 (2005), pp. 14026-14038
- [14] Y. Xiao, Z. Wang, K. Ding Macromolecules, 39 (2006), pp. 128-137
- [15] H. Sugimoto, H. Ohshima, S. Inoue J Polym Sci Part A Polym Chem, 41 (2003), pp. 3549-3555
- [16] D.J. Darensbourg, D.R. Billodeaux Inorg Chem, 44 (2005), pp. 1433-1442
- [17] A. Buchard, M.R. Kember, K.G. Sandeman, C.K. Williams Chem Commun, 47 (2011), pp. 212-214

- [18] K. Nakano, K. Kobayashi, T. Ohkawara, H. Imoto, K. Nozaki *J Am Chem Soc*, 135 (2013), pp. 8456-8459
- [19] Z. Quan, X. Wang, X. Zhao, F. Wang *Polymer*, 44 (2003), pp. 5605-5610
- [20] B. Liu, X. Zhao, X. Wang, F. Wang *J Polym Sci Part A Polym Chem*, 39 (2001), pp. 2751-2754
- [21] D. Cui, M. Nishiura, Z. Hou *Macromolecules*, 38 (2005), pp. 4089-4095
- [22] X.-B. Lu, D.J. Darensbourg *Chem Soc Rev*, 41 (2012), pp. 1462-1484
- [23] X.-B. Lu, L. Shi, Y.-M. Wang, R. Zhang, Y.-J. Zhang, X.-J. Peng, et al. *J Am Chem Soc*, 128 (2006), pp. 1664-1674
- [24] C.T. Cohen, G.W. Coates *J Polym Sci Part A Polym Chem*, 44 (2006), pp. 5182-5191
- [25] K. Nakano, S. Hashimoto, M. Nakamura, T. Kamada, K. Nozaki *Angew Chem Int Ed*, 50 (2011), pp. 4868-4871
- [26] X.-B. Lu, Y. Wang *Angew Chem Int Ed*, 43 (2004), pp. 3574-3577
- [27] G.A. Luinstra, G.R. Haas, F. Molnar, V. Bernhart, R. Eberhardt, B. Rieger *Chem Eur J*, 11 (2005), pp. 6298-6314
- [28] P.P. Pescarmona, M. Taherimehr *Catal Sci Technol*, 2 (2012), pp. 2169-2187
- [29] D.J. Darensbourg *Chem Rev*, 107 (2007), pp. 2388-2410
- [30] E.K. Noh, S.J. Na, S. Sujith, S.-W. Kim, B.Y. Lee *J Am Chem Soc*, 129 (2007), pp. 8082-8083
- [31] S.S.J.K. Min, J.E. Seong, S.J. Na, B.Y. Lee *Angew Chem Int Ed*, 47 (2008), pp. 7306-7309
- [32] C.T. Cohen, T. Chu, G.W. Coates *J Am Chem Soc*, 127 (2005), pp. 10869-10878
- [33] W.-M. Ren, Z.-W. Liu, Y.-Q. Wen, R. Zhang, X.-B. Lu *J Am Chem Soc*, 131 (2009), pp. 11509-11518
- [34] X.-B. Lu, W.-M. Ren, G.-P. Wu *Acc Chem Res*, 45 (2012), pp. 1721-1735
- [35] M.I. Childers, J.M. Longo, N.J. Van Zee, A.M. LaPointe, G.W. Coates *Chem Rev*, 114 (2014), pp. 8129-8152
- [36] W.M. Ren, W.Z. Zhang, X.B. Lu *Sci China Chem*, 53 (2010), pp. 1646-1652
- [37] W.-M. Ren, Y. Liu, G.-P. Wu, J. Liu, X.-B. Lu *J Polym Sci Part A Polym Chem*, 49 (2011), pp. 4894-4901
- [38] Y. Liu, W.-M. Ren, J. Liu, X.-B. Lu *Angew Chem Int Ed*, 52 (2013), pp. 11594-11598
- [39] K.A. Salmeia, S. Vagin, C.E. Anderson, B. Rieger *Macromolecules*, 45 (2012), pp. 8604-8613
- [40] C.J. Whiteoak, G. Salassa, A.W. Kleij *Chem Soc Rev*, 41 (2012), pp. 622-631
- [41] D.J. Darensbourg, P. Ganguly, D. Billodeaux *Macromolecules*, 38 (2005), pp. 5406-5410
- [42] H. Sugimoto, H. Ohtsuka, S. Inoue *J Polym Sci Part A Polym Chem*, 43 (2005), pp. 4172-4186
- [43] L.-J. Chen, J. Bao, F.-M. Mei, G.-X. Li *Catal Commun*, 9 (2008), pp. 658-663
- [44] R. Reichardt, S. Vagin, R. Reithmeier, A.K. Ott, B. Rieger *Macromolecules*, 43 (2010), pp. 9311-9317
- [45] H. Ajiro, K.L. Peretti, E.B. Lobkovsky, G.W. Coates *Dalton Trans* (2009), pp. 8828-8830
- [46] C.T. Cohen, C.M. Thomas, K.L. Peretti, E.B. Lobkovsky, G.W. Coates *Dalton Trans* (2006), pp. 237-249
- [47] S. Klaus, S.I. Vagin, M.W. Lehenmeier, P. Deglmann, A.K. Brym, B. Rieger *Macromolecules*, 44 (2011), pp. 9508-9516
- [48] Y. Wang, Y. Qin, X. Wang, F. Wang *ACS Catal*, 5 (2015), pp. 393-396
- [49] L. Shi, X.-B. Lu, R. Zhang, X.-J. Peng, C.-Q. Zhang, J.-F. Li, et al. *Macromolecules*, 39 (2006), pp. 5679-5685
- [50] K. Nakano, T. Kamada, K. Nozaki *Angew Chem Int Ed*, 45 (2006), pp. 7274-7277
- [51] A. Cyriac, S.H. Lee, J.K. Varghese, E.S. Park, J.H. Park, B.Y. Lee *Macromolecules*, 43 (2010), pp. 7398-7401
- [52] K.L. Peretti, H. Ajiro, C.T. Cohen, E.B. Lobkovsky, G.W. Coates *J Am Chem Soc*, 127 (2005), pp. 11566-11567

## SUPPORTING INFORMATION

### Salphen-Co(III) complexes catalyzed copolymerization of epoxides with CO<sub>2</sub>

Zdeněk Hošťálek<sup>a,d</sup>, Robert Mundil<sup>a</sup>, Ivana Císařová<sup>b</sup>, Olga Trhlíková<sup>c</sup>, Etienne Grau<sup>d</sup>, Frederic Peruch<sup>d</sup>, Henri Cramail<sup>d</sup> and Jan Merna<sup>a,\*</sup>

<sup>a</sup> Institute of Chemical Technology, Prague, Department of Polymers, Technická 5, 166 28 Prague 6, Czech Republic.

<sup>b</sup> Department of Inorganic Chemistry, Faculty of Science, Charles University in Prague, Hlavova 2030, 12840 Prague 2, Czech Republic

<sup>c</sup> Institute of Macromolecular Chemistry of the ASCR, v.v.i, Heyrovského náměstí 2, 162 06 Praha 6, Czech Republic

<sup>d</sup> Laboratoire de Chimie des Polymeres Organiques, UMR5629, Univ. Bordeaux, CNRS, INPB-ENSCBP, 16, Avenue Pey Berland, Pessac Cedex, F-33607, France

Content:

1. Evaluation of $Y_w$ , TOF to polymer and TOF to cyclic carbonate	S1
2. Correlation of molar masses obtained with SEC-MALLS and SEC-PS calibration method	S2
3. SEC chromatograms of poly(propylene carbonate) polymers	S2
4. NMR characterization of complex 3	S3
5. Characterization of complex 2a	S7
6. Characterization of complex 2b	S8
7. Characterization of complex 2c	S10
8. Characterization of complex 3a	S12
9. Characterization of complex 3b	S14
10. Characterization of complex 3d	S16
11. Crystal data of complex 2c	S16

#### 1. Evaluation of $Y_w$ , TOF to polymer and TOF to cyclic carbonate

Yield was calculated by using equation (1),

$$(1) Y_w = m_{\text{POLYMER}} \times \frac{M_{\text{EPOXIDE}}}{M_{\text{RU}}} / m_{\text{EPOXIDE}}$$

where  $m_{\text{POLYMER}}$  and  $m_{\text{EPOXIDE}}$  is mass of isolated polymer and epoxide in feed, respectively,  $M_{\text{EPOXIDE}}$  is molar mass of monomer unit and  $M_{\text{RU}}$  corresponds to molar mass of repeating (carbonate) unit in polymer.

Turnover frequency to polymer was calculated using formula (2):

$$(2) \text{TOF}_{\text{POL}} = \frac{m_{\text{POLYMER}}}{M_{\text{RU}} \times n_{\text{CAT}} \times t_p};$$

Where  $n_{\text{CAT}}$  is molar amount of catalyst and  $t_p$  is time of polymerization.

Turnover frequency to cyclic carbonate (CC) was calculated from equation (3):

$$(3) \text{TOF}_{\text{CC}} = \frac{m_{\text{CC}}}{M_{\text{CC}} \times n_{\text{CAT}} \times t_p}$$

where  $m_{\text{CC}}$  is mass of cyclic carbonate calculated according to (4):

$$(4) m_{\text{CC}} = (m_{\text{EPOXIDE}} - (m_{\text{EPOXIDE}} \times Y_{\text{W POL}})) \times \frac{I_{\text{CH}}(\text{CC})}{I_{\text{CH}}(\text{CC}) + I_{\text{CH}}(\text{EPOXIDE})}$$

where  $I_{\text{CH}}(\text{CC})$  and  $I_{\text{CH}}(\text{EPOXIDE})$ , are integrals of <sup>1</sup>H NMR signals of methine groups present in cyclic carbonate and epoxide respectively.

## 2. Correlation of molar masses obtained with SEC-MALLS and SEC-PS calibration method

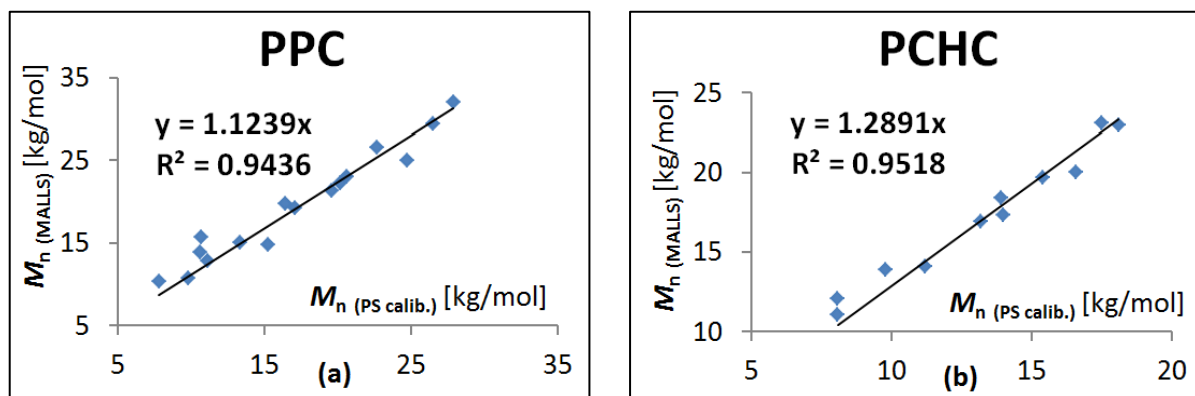


Figure S1: Correlation of molar masses of PPC (a) and PCHC (b) obtained by SEC-MALLS and PS calibration method

## 3. SEC chromatograms of poly(propylene carbonate) polymers

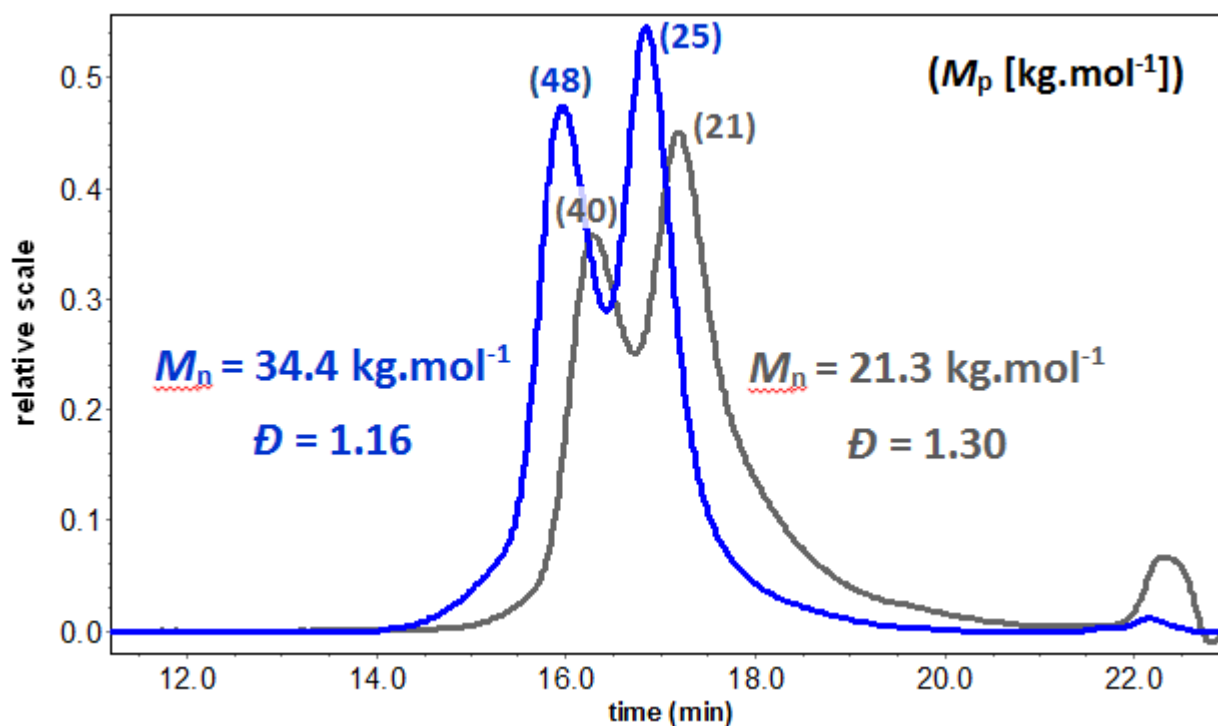
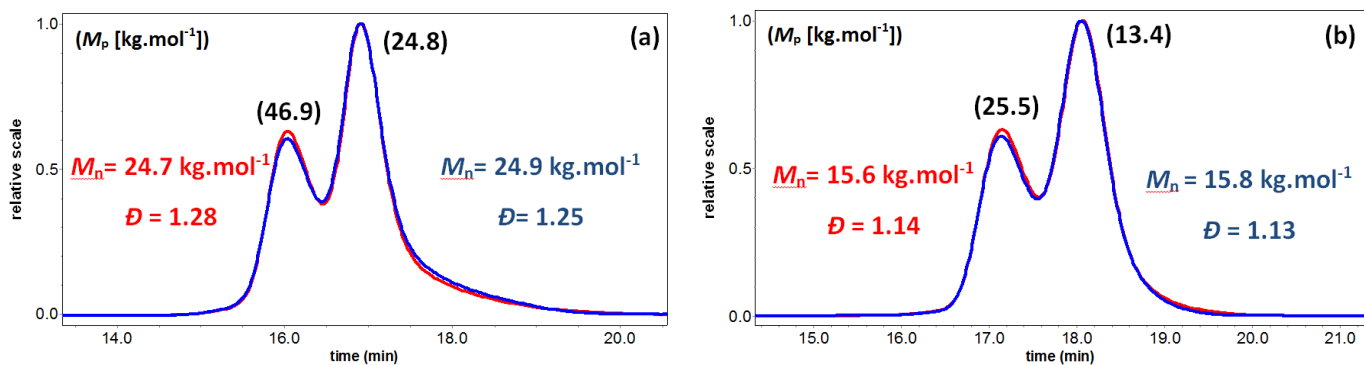
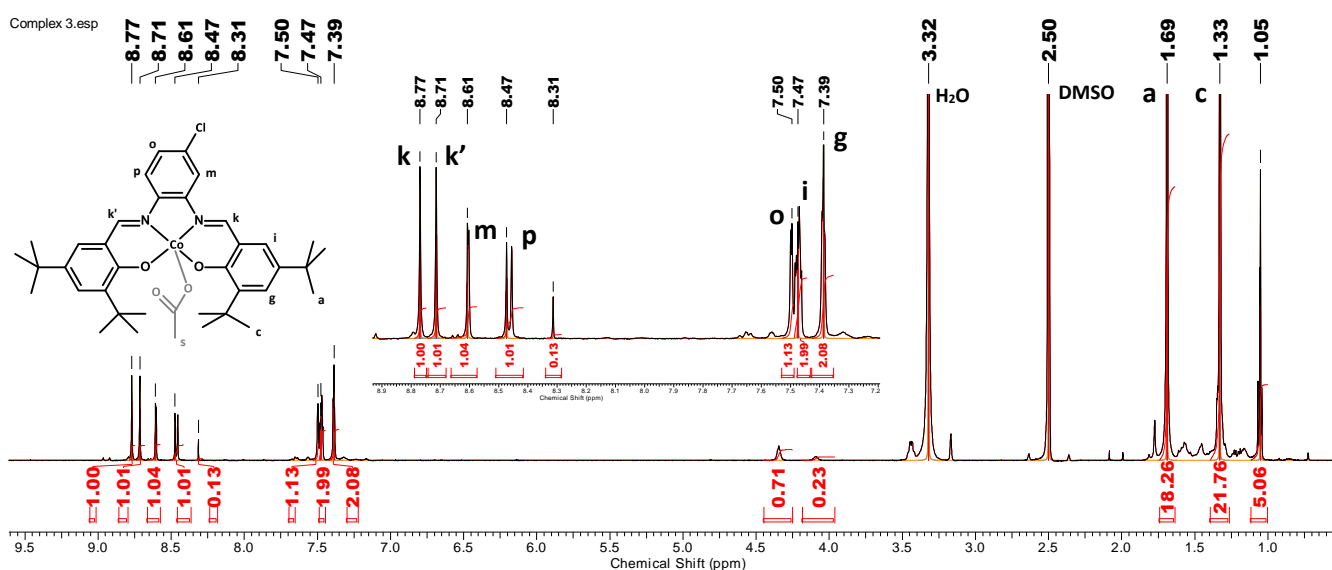


Figure S2: SEC chromatograms (RI-detection) of poly(propylene carbonate)s obtained with catalyst 2a (exp. 2 - blue) and 2b (exp. 7 - grey)



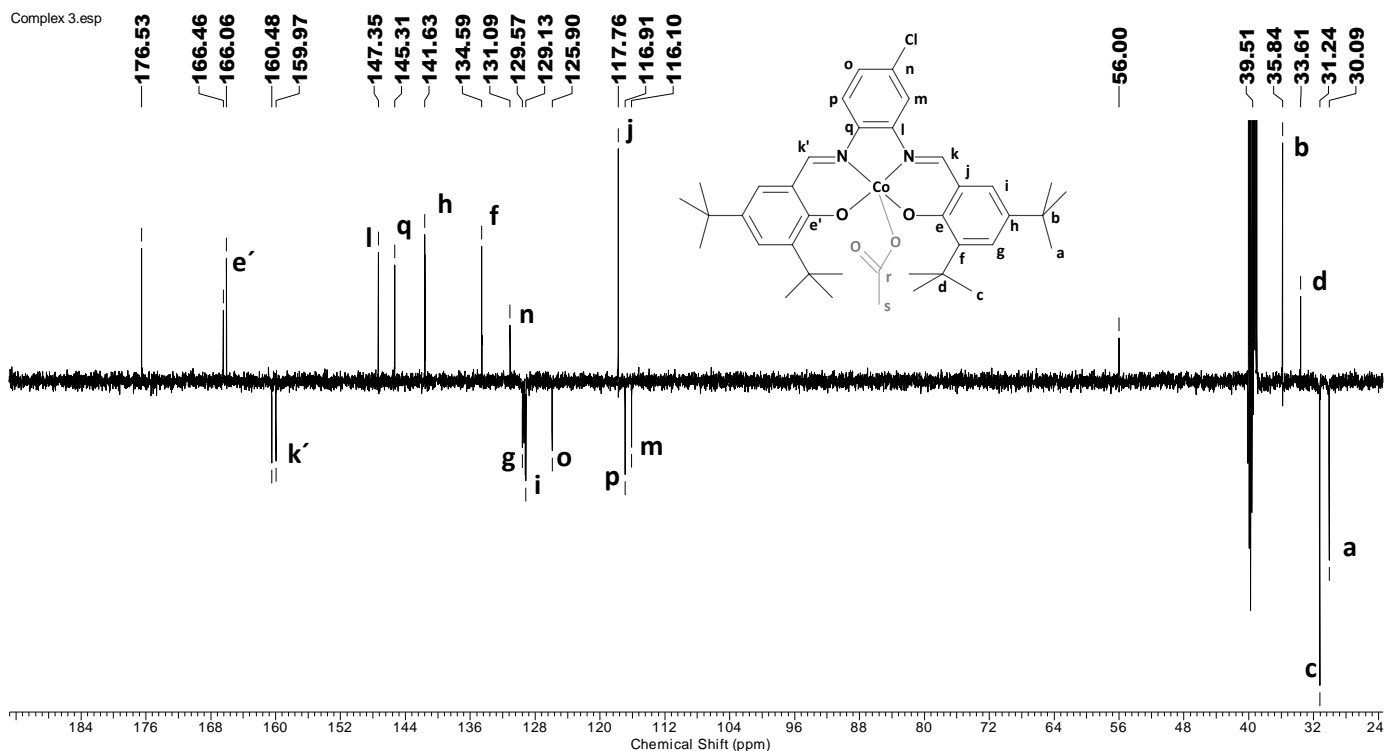
**Figure S3:** SEC chromatograms (RI-detection) of poly(propylenecarbonate) (a) and poly(cyclohexenecarbonate) (b) before hydrolysis (red line) and after hydrolysis in 1M HCl<sub>DCM sol.</sub> (blue line)

#### 4. NMR characterization of complex 3

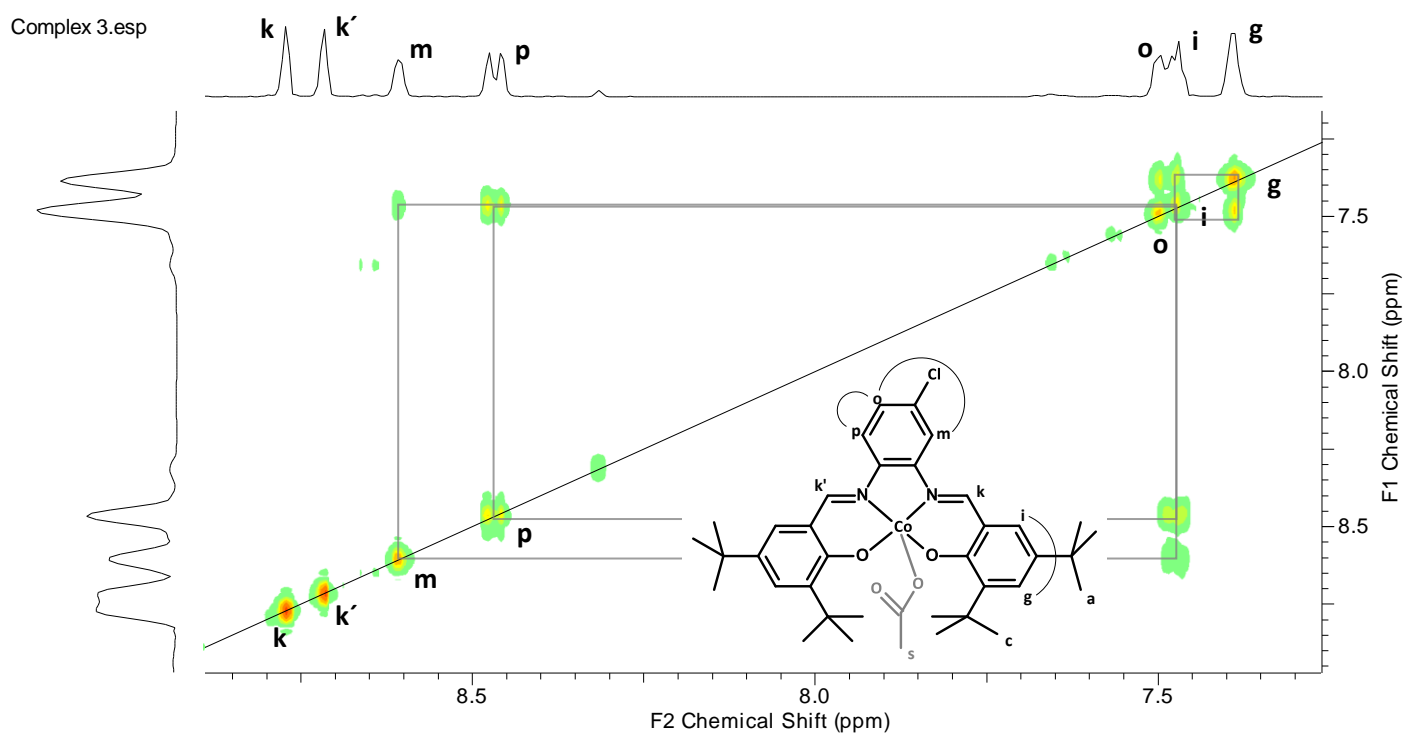


**Figure S4:** <sup>1</sup>H NMR of complex 3 in DMSO

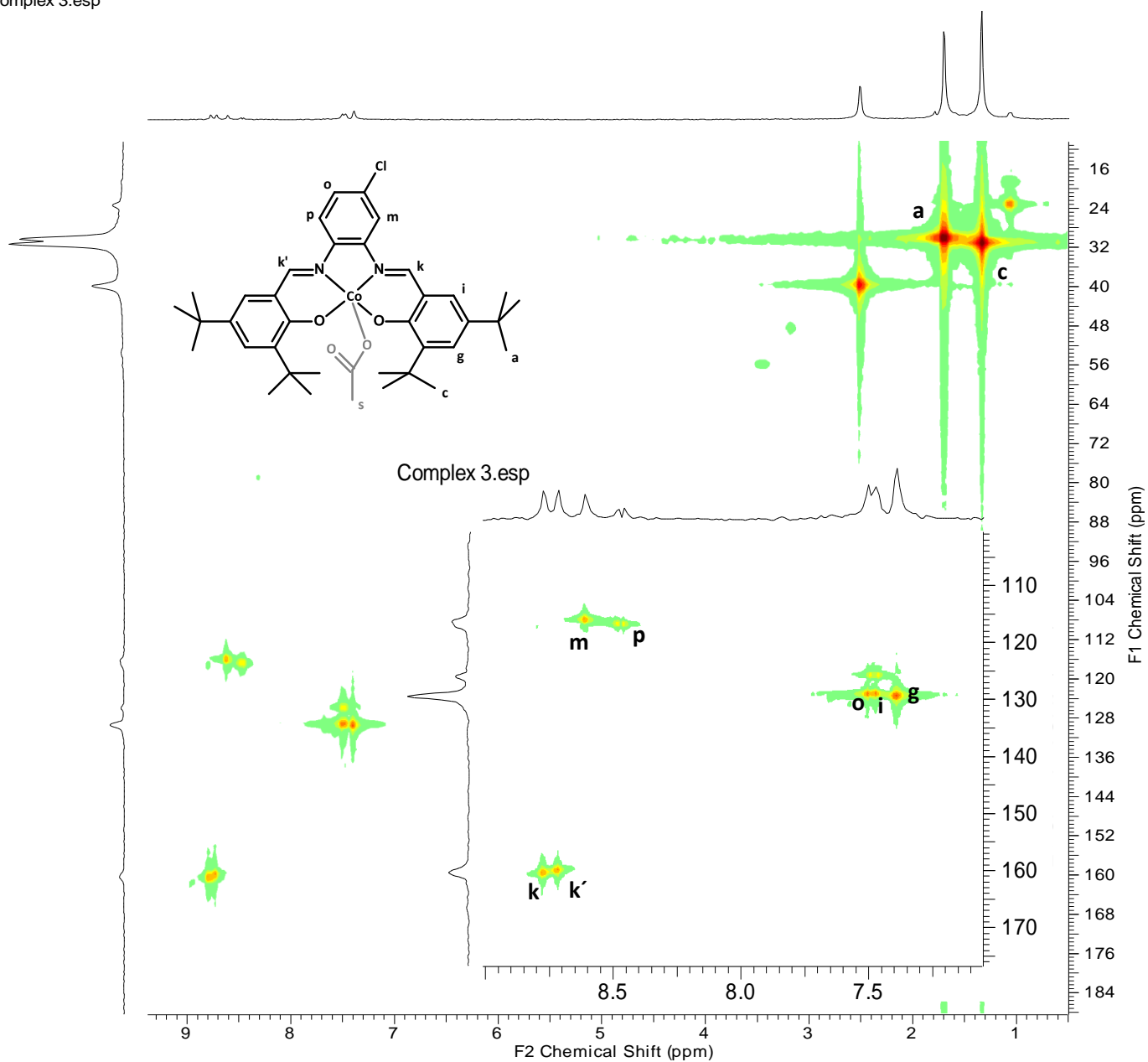
<sup>1</sup>H NMR (DMSO-d<sub>6</sub>, 500 MHz):  $\delta$  1.33 (18H, -CH<sub>3</sub> (b)), 1.69 (s, 18H, -CCH<sub>3</sub> (a)), 7.39 (2H, =CH- (g)); 7.47 (2H, ArH (i)), 7.50 (1H, ArH (o)), 8.47 (1H, ArH (p)), 8.61 (1H, ArH (m)), 8.71 (1H, -N=CH- (k')), 8.77 (1H, -N=CH- (k)).

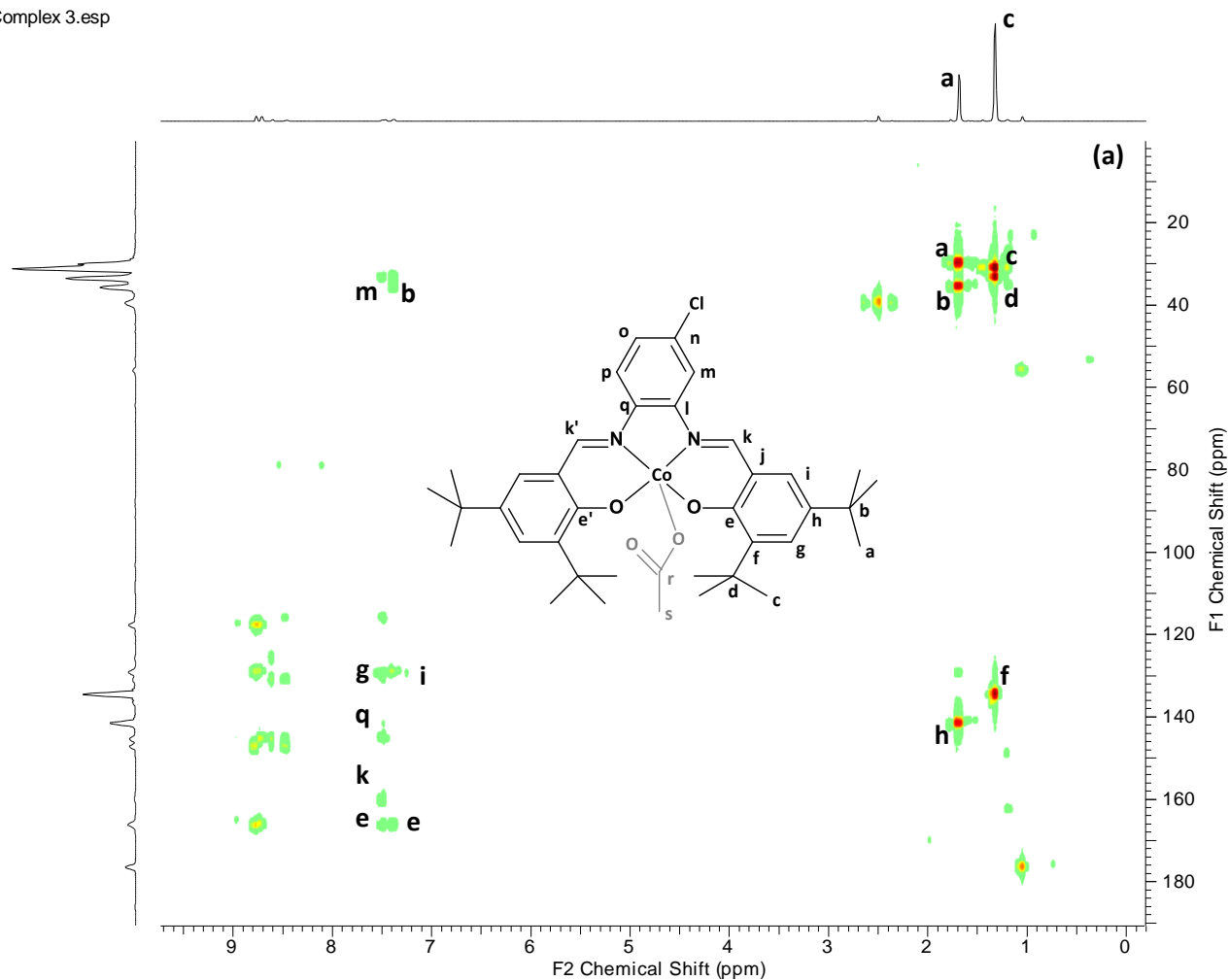


$^1\text{H}$  NMR (DMSO- $d_6$ , 500 MHz): 30.09 ( $-\text{CH}_3$  (a)), 31.24 ( $-\text{CH}_3$  (c)), 33.61 ( $-\text{C}(\text{CH}_3)_3$  (d)), 35.84 ( $-\text{C}(\text{CH}_3)_3$  (b)), 116.10 ( $=\text{CH}-\text{Ar}$ , (m)), 116.91 ( $=\text{CH}-\text{Ar}$ , (p)), 117.76 ( $=\text{C}-\text{Ar}$ , (j)), 125.90 ( $=\text{C}-\text{Ar}$ , (o)), 129.13 ( $=\text{CH}-\text{Ar}$ , (i)), 129.57 ( $=\text{CH}-\text{Ar}$ , (g)), 131.09 ( $=\text{CCl}-\text{Ar}$  (n)), 134.59 ( $=\text{C}-\text{Ar}$  (f)), 141.63 ( $=\text{C}-\text{Ar}$  (h)), 145.31 ( $=\text{C}-\text{Ar}$ , (q)), 147.35 ( $=\text{C}-\text{Ar}$ , (l)), 159.97 ( $-\text{N}=\text{CH}-$ , (k')), 160.48 ( $-\text{N}=\text{CH}-$ , (k)), 166.06 ( $=\text{C}-\text{O}-\text{Ar}$  (e')), 166.46 ( $=\text{C}-\text{O}-\text{Ar}$  (e)).



Complex 3.esp





Complex 3.esp

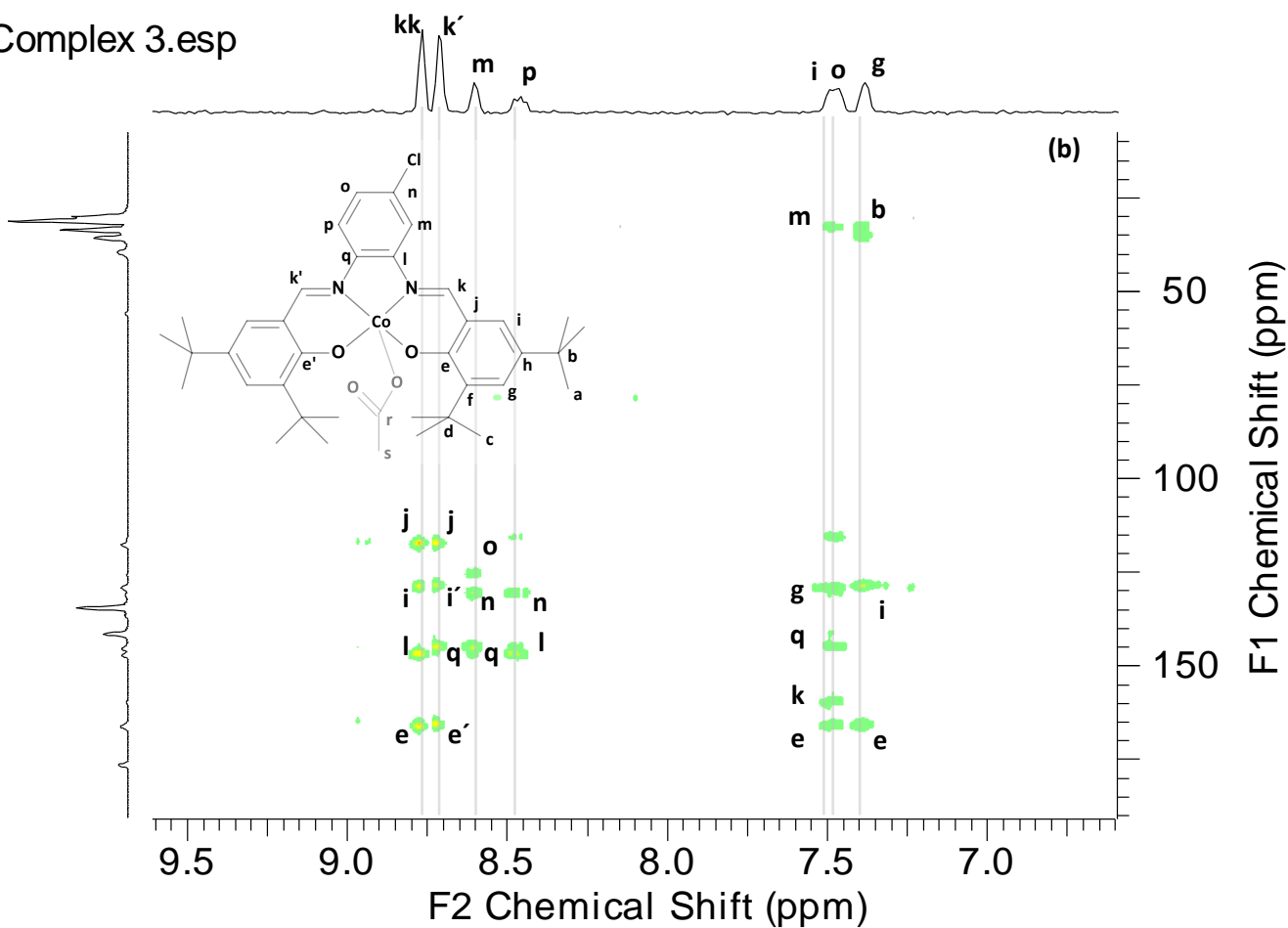


Figure S8 (a) HMBC NMR of complex 3, (b) expansion of region 6.5 ppm – 9.5 ppm

## 5. Characterization of complex 2a

1\_Hostalek\_ZH438\_1#49-60\_RT:0.73-0.89\_AV:12\_NL:8.63E6  
T: FTMS + c ESI Full ms [130.00-1500.00]

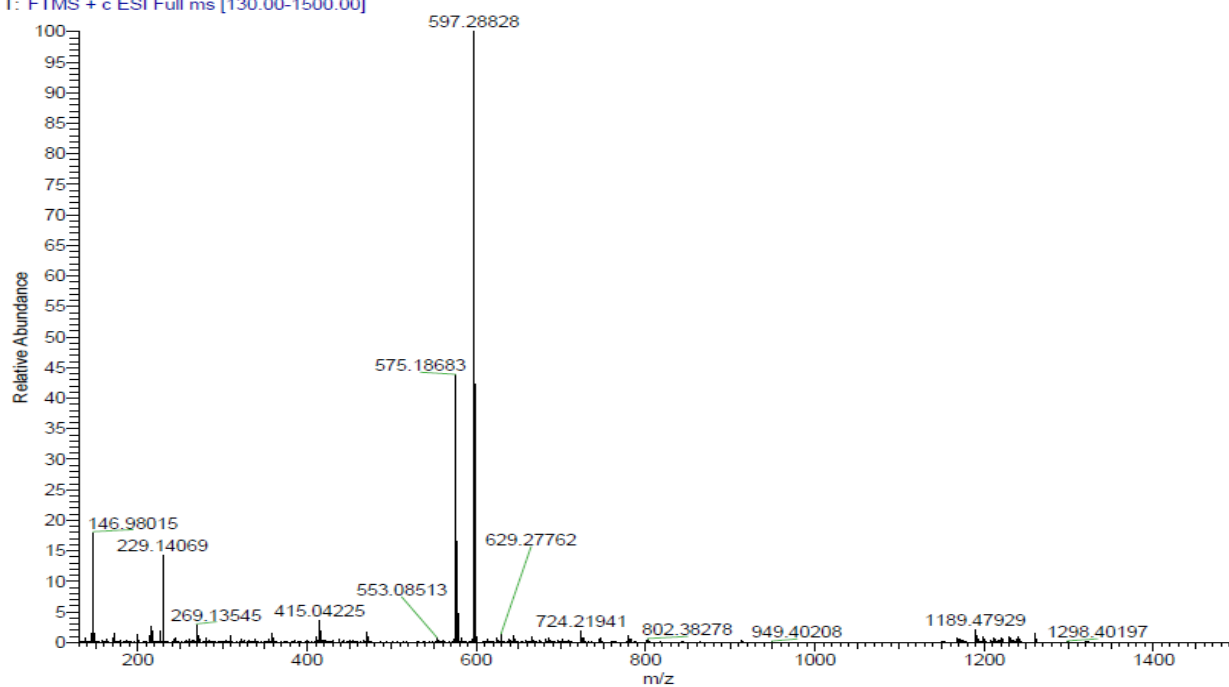


Figure S9: HRMS-ESI<sup>+</sup> spectrum of complex 2a

1\_Hostalek\_ESIneg\_ZH438\_1#81\_RT:1.81\_AV:1\_NL:2.14E6  
T: FTMS - c ESI Full ms [110.00-1000.00]

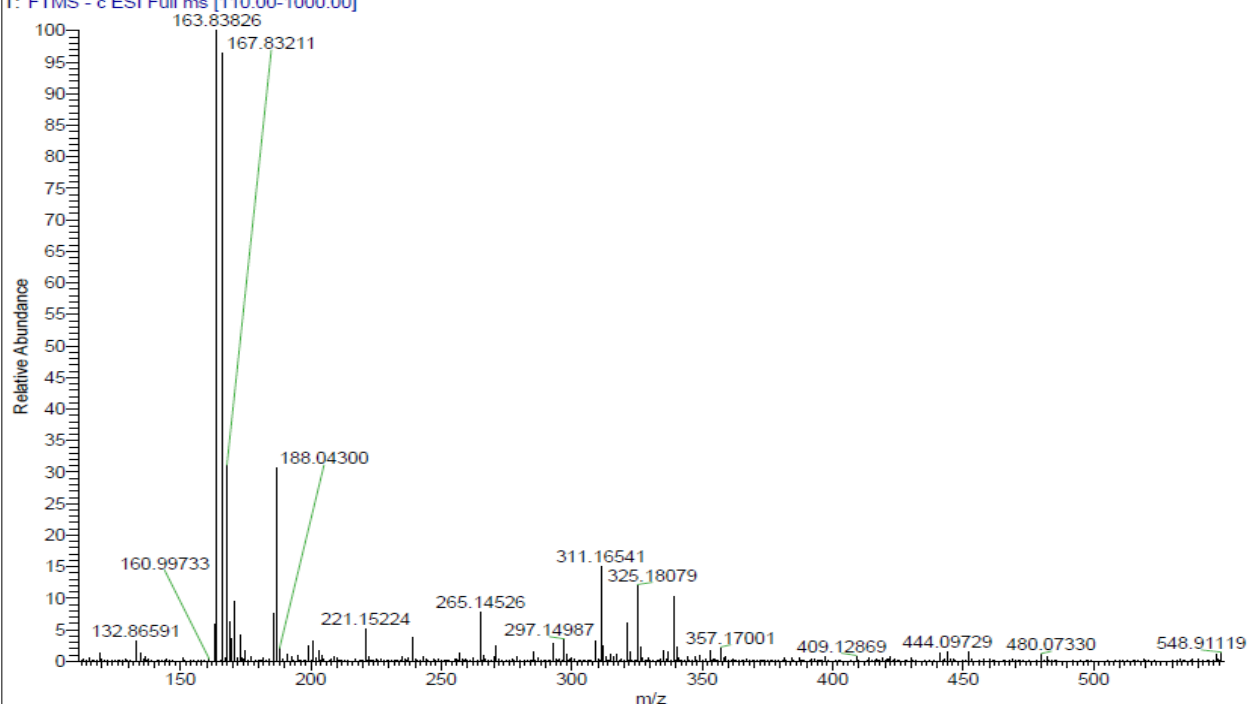


Figure S10: HRMS-ESI<sup>-</sup> spectrum of complex 2a

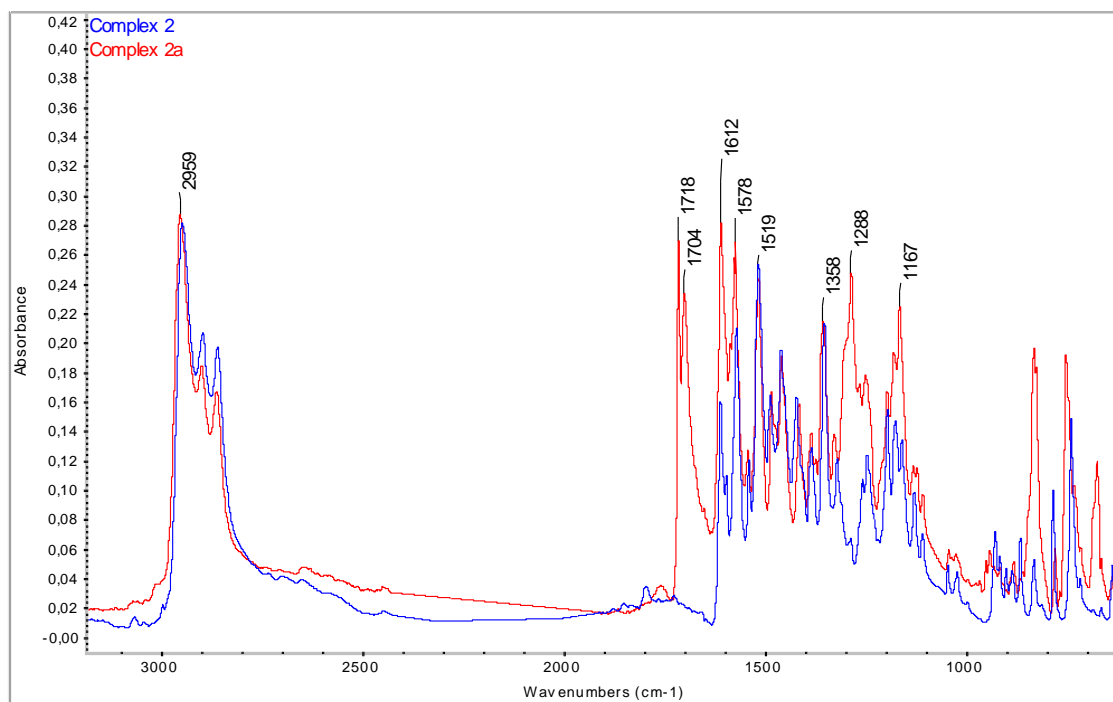


Figure S11: FT-IR spectra of complexes **2** and **2a**

## 6. Characterization of complex **2b**

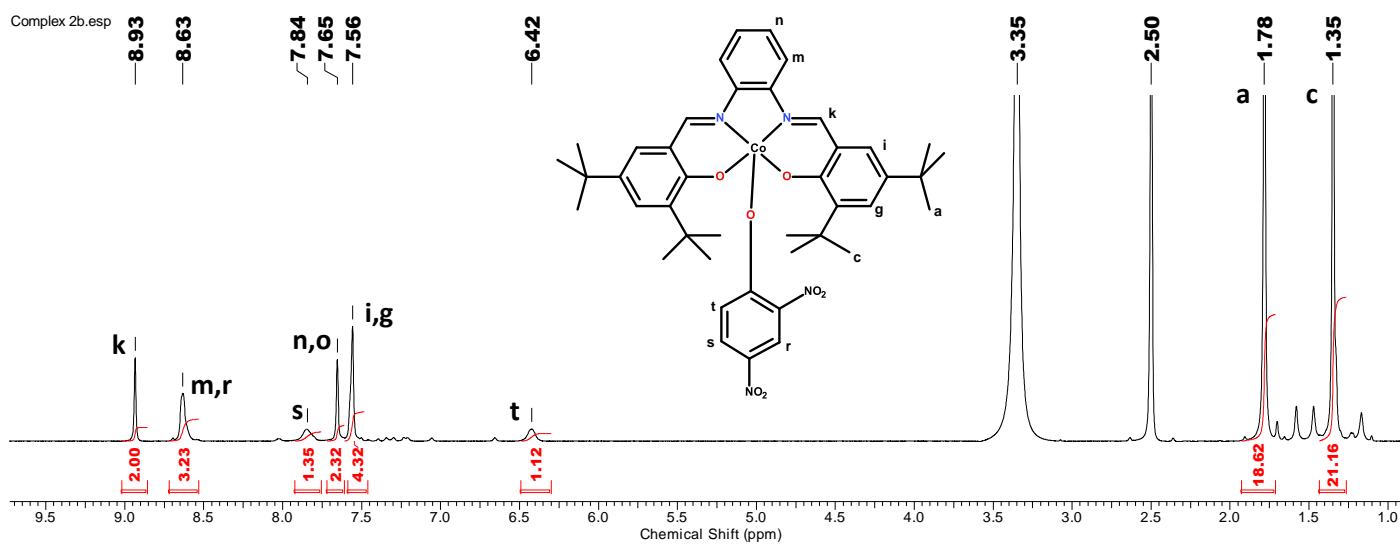


Figure S12:  $^1\text{H}$  NMR of complex **2b** in DMSO

$^1\text{H}$  NMR (DMSO- $d_6$ , 500 MHz):  $\delta$  1.35 (18H,  $-\text{CH}_3$  (c)), 1.78 (s, 18H,  $-\text{CCH}_3$  (a)), 6.42 (1H, ArH (DNP)), 7.56 (4H, ArH (i,g)), 7.65 (2H, ArH (n)), 7.84 (1H, ArH (DNP)), 8.63 (3H, ArH (m+DNP)), 8.93 (2H,  $-\text{N}=\text{CH}$ -(k)).

214 Hostalek ESIpos ZH436 1 #119-127 RT: 1.78-1.91 AV: 9 NL: 1.01E7  
T: FTMS + c ESI Full ms [100.00-1500.00]

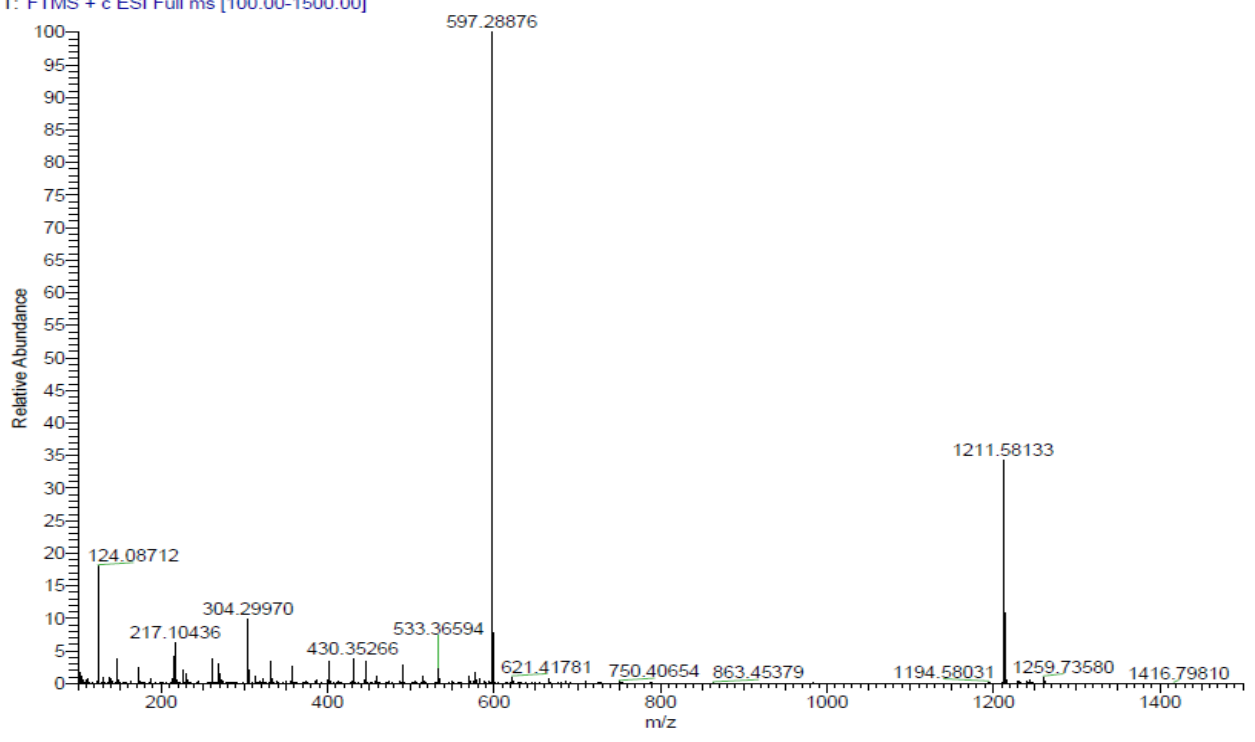


Figure S13: HRMS-ESI<sup>+</sup> spectrum of complex 2b

214 hostalek esineq zh436 4 recal #97 RT: 2.29 AV: 1 NL: 1.08E7  
T: FTMS - c ESI Full ms [80.00-1000.00]

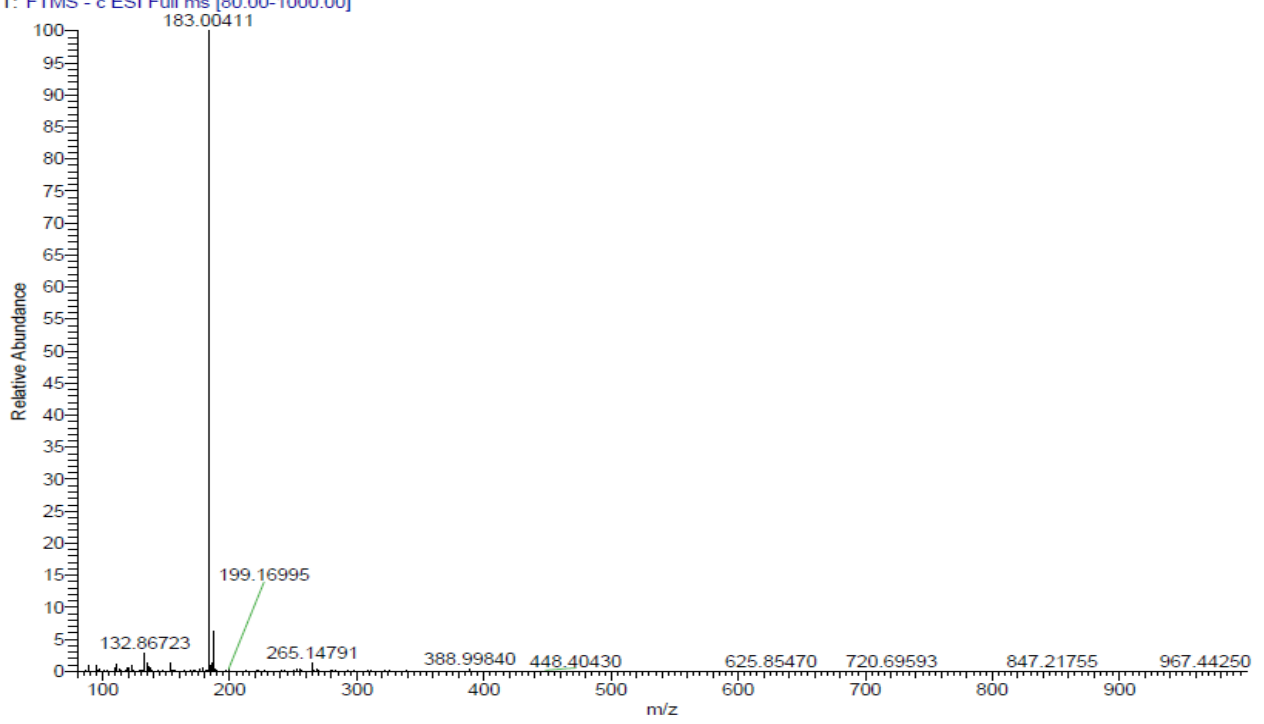


Figure S14: HRMS-ESI<sup>-</sup> spectrum of complex 2b

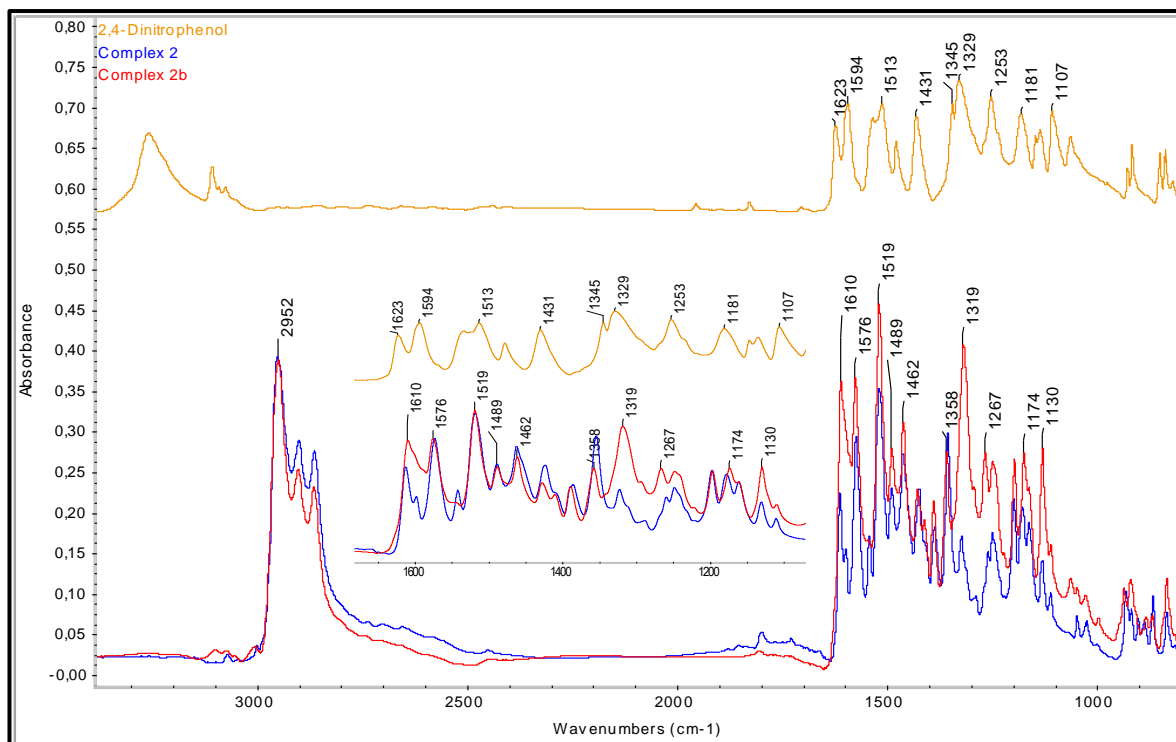


Figure S15: FT-IR spectra of complexes **2** and **2b**

## 7. Characterization of complex **2c**

334 Hostalek\_ZH485\_1 #143-152 RT: 1.46-1.59 AV: 10 NL: 3.97E7  
T: FTMS + c ESI Full ms [140.00-2000.00]

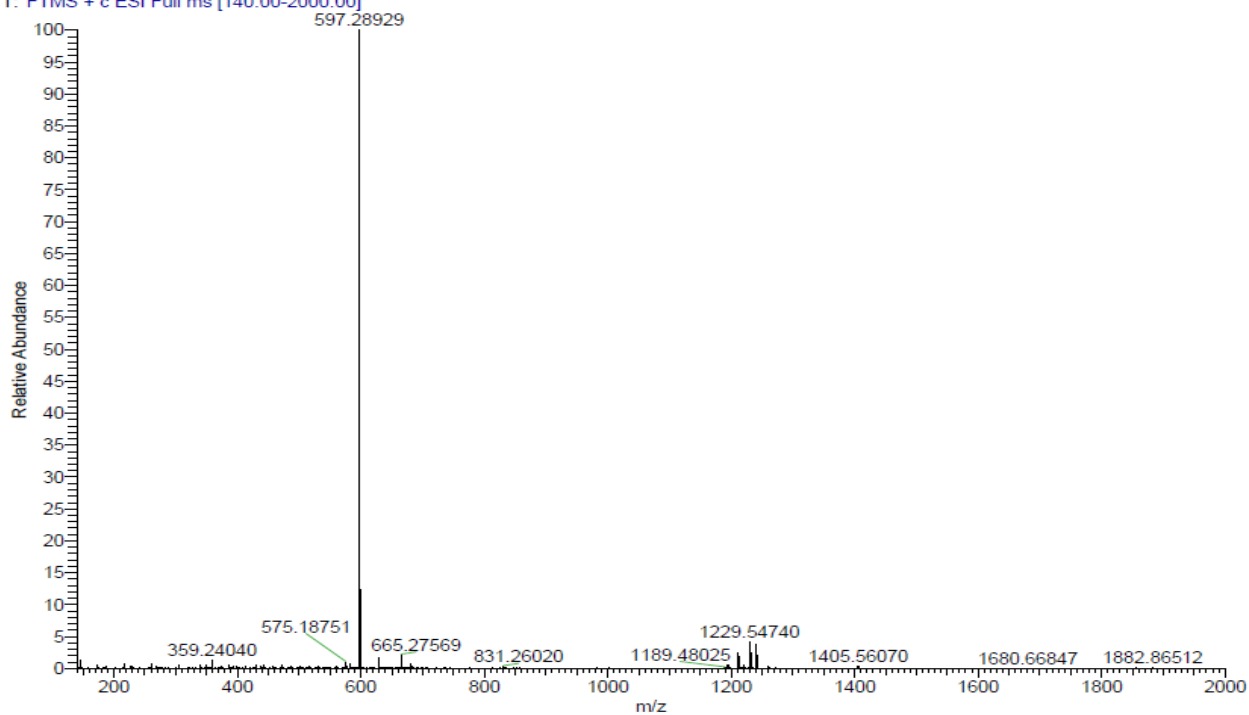


Figure S16: HRMS-ESI<sup>+</sup> spectrum of complex **2c**

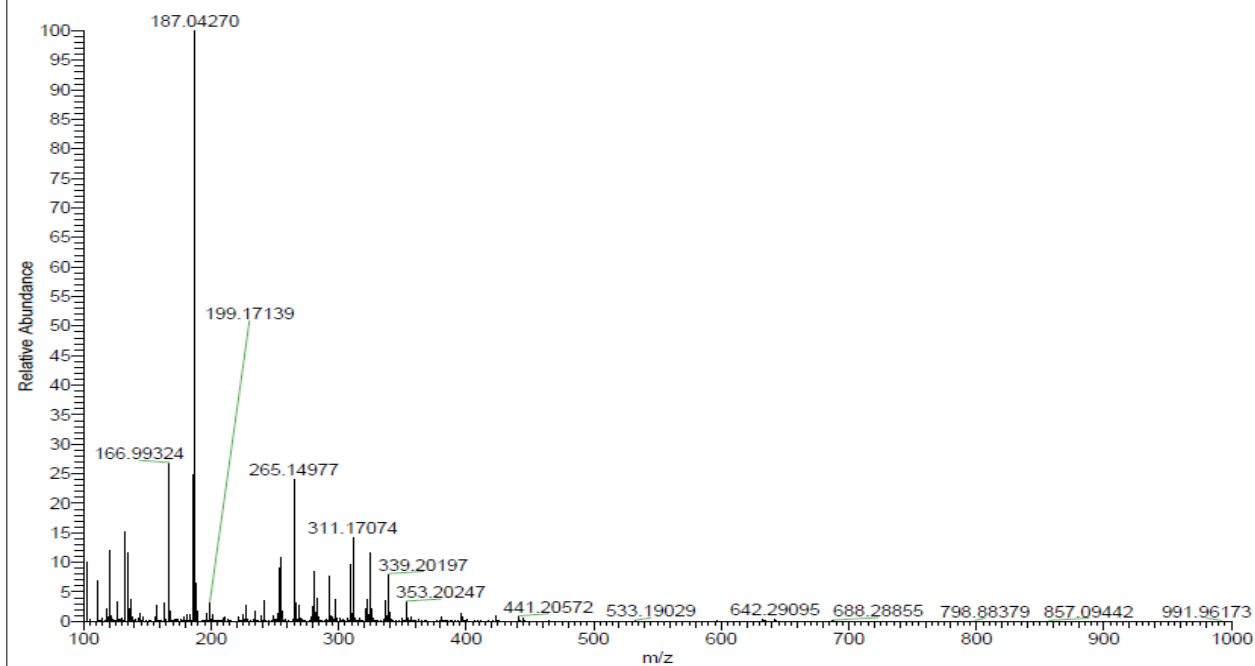


Figure S17: HRMS-ESI<sup>+</sup> spectrum of complex 2c

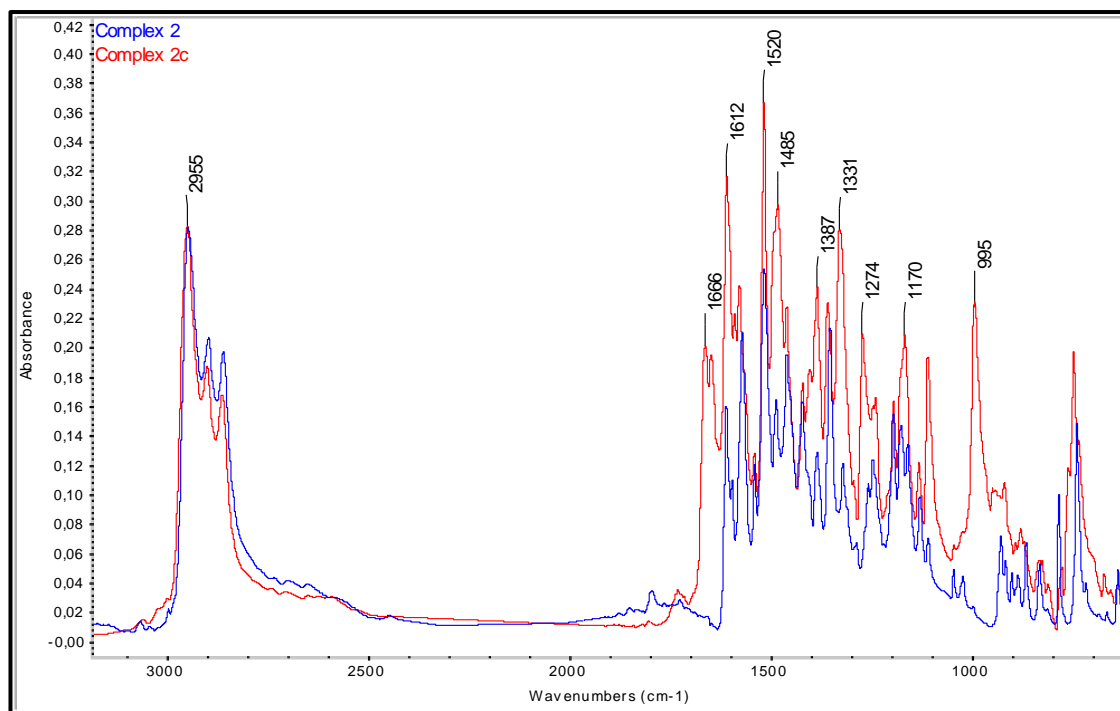
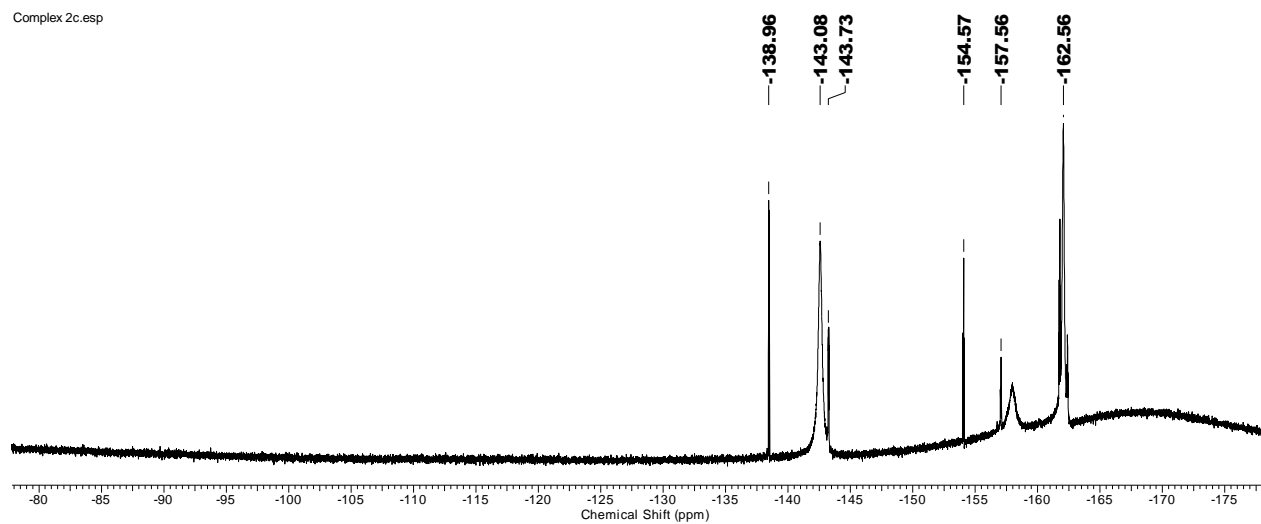
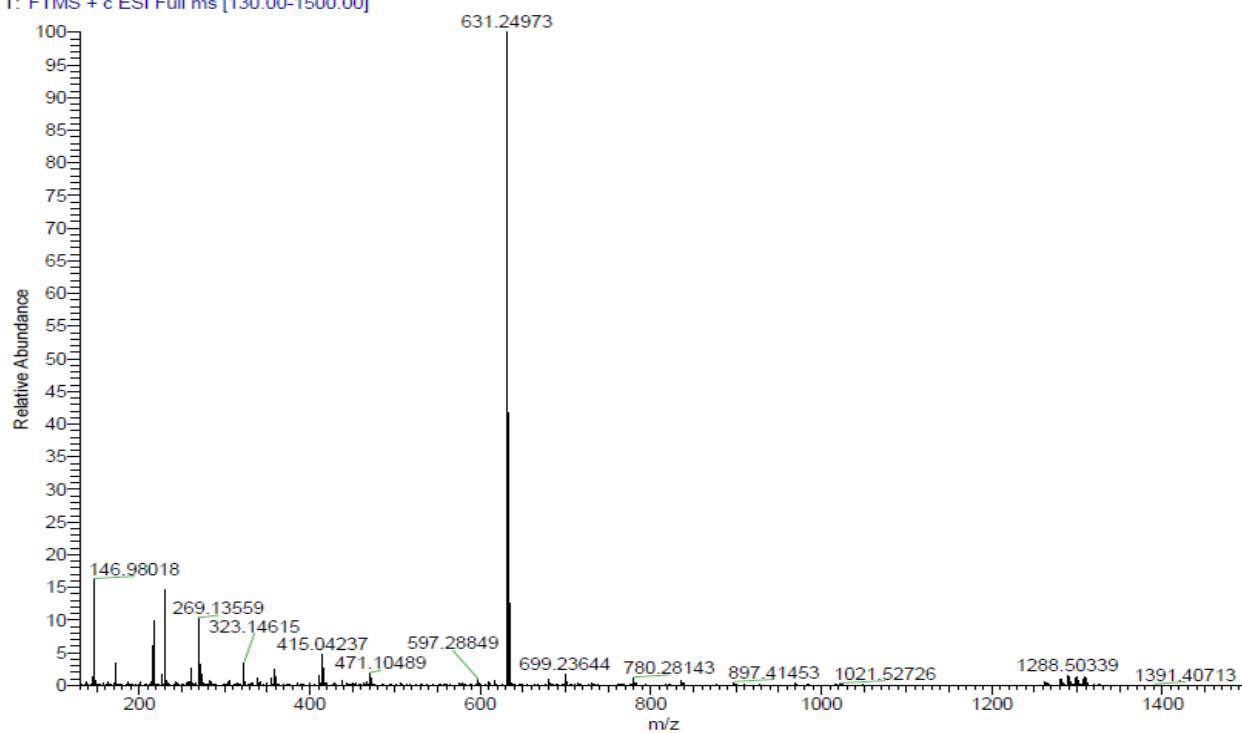


Figure S18: FT-IR spectra of complexes 2 and 2c

Figure S19:  $^{19}\text{F}$  NMR of complex 2c

## 8. Characterization of complex 3a

1\_Hostalek\_ZH439\_1 #56-63 RT: 0.83-0.94 AV: 8 NL: 1.13E7  
T: FTMS + c ESI Full ms [130.00-1500.00]

Figure S20: HRMS-ESI<sup>+</sup> spectrum of complex 3a

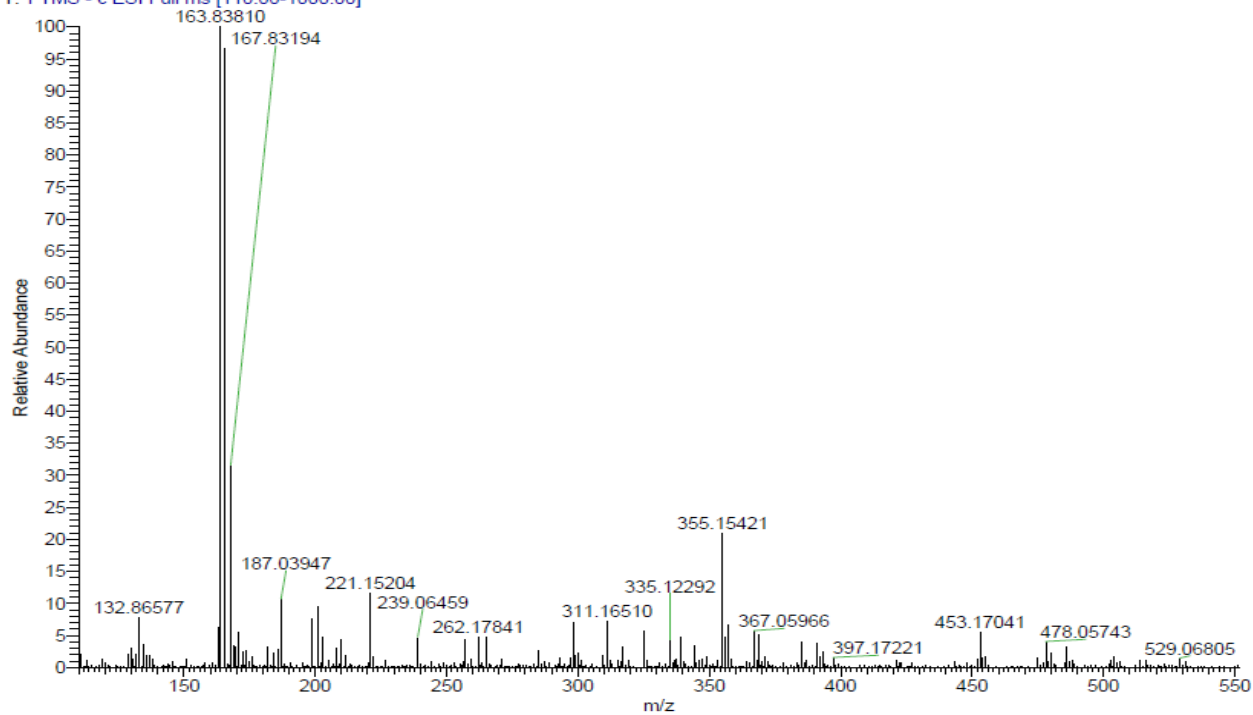


Figure S21: HRMS-ESI spectrum of complex 3a

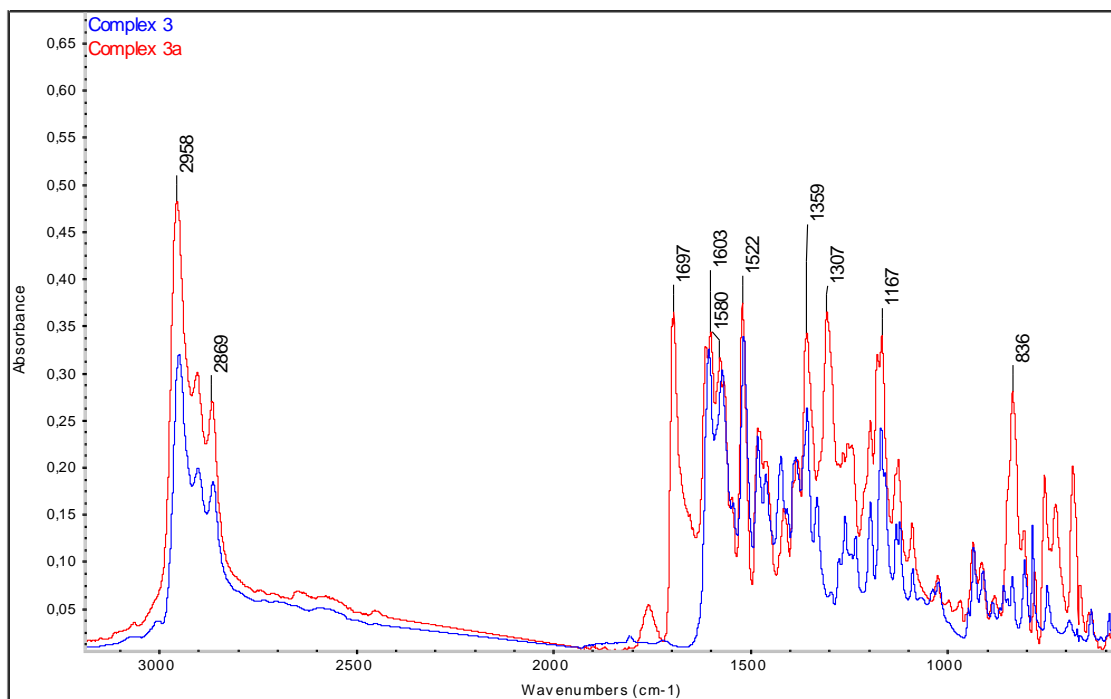


Figure S22: FT-IR spectra of complexes 3 and 3a

## 9. Characterization of complex 3b

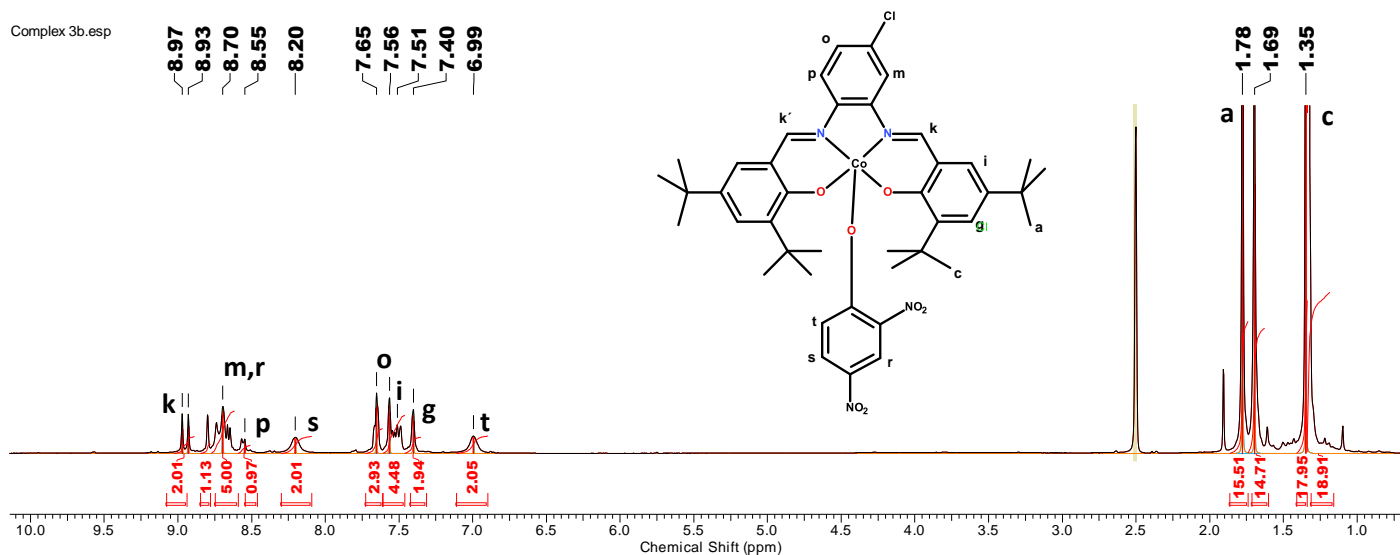


Figure S23:  $^1\text{H}$  NMR of complex 3b in DMSO

$^1\text{H}$  NMR (DMSO- $d_6$ , 500 MHz):  $\delta$  1.35 (18H,  $-\text{CH}_3$  (b)), 1.78 (s, 18H,  $-\text{CCH}_3$  (a)), 6.99 (1H, ArH (DNP)), 7.40 (2H,  $=\text{CH}-$  (g)); 7.51 (2H, ArH (i)), 7.56 (1H, ArH (o)), 8.20 (1H, ArH (DNP)), 8.55 (1H, ArH (p)), 8.70 (1H, ArH (m+DNP)), 8.93 (1H,  $-\text{N}=\text{CH}-$  (k)), 8.97 (1H,  $-\text{N}=\text{CH}-$  (k')).

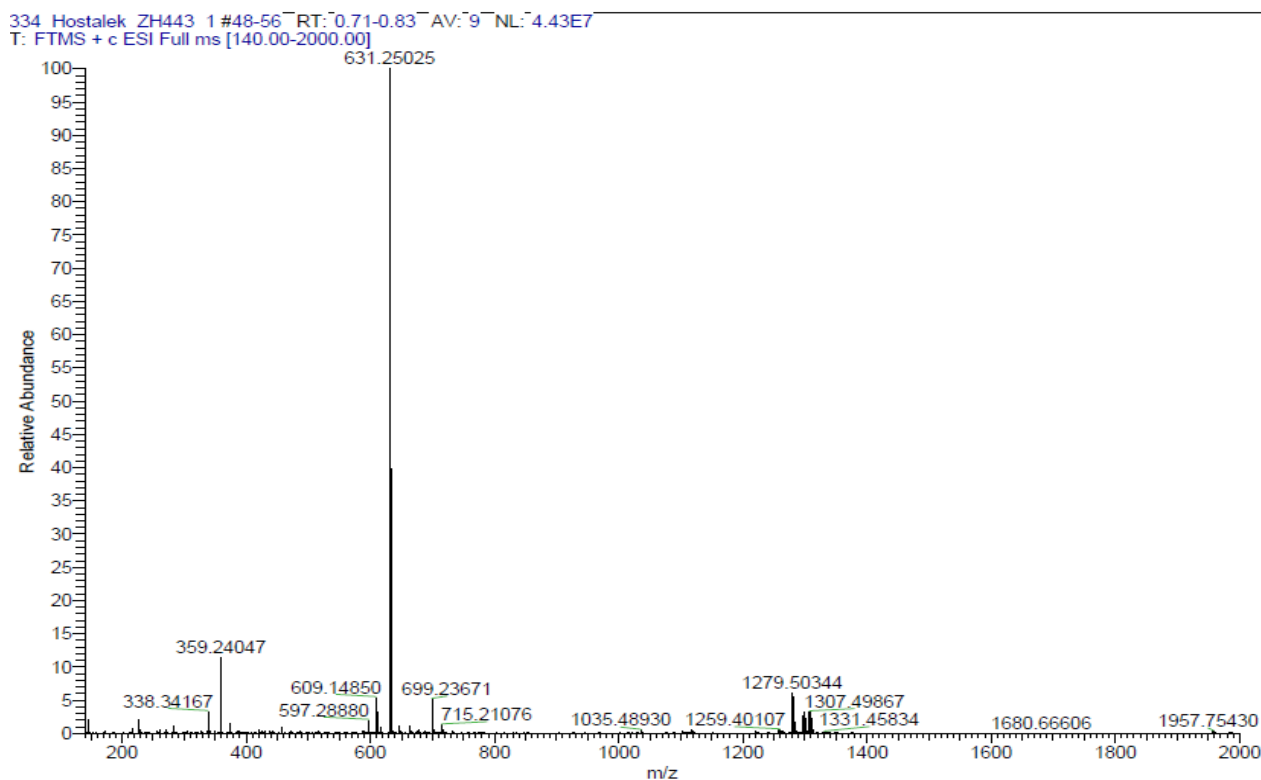


Figure S24: HRMS-ESI $^+$  spectrum of complex 3b

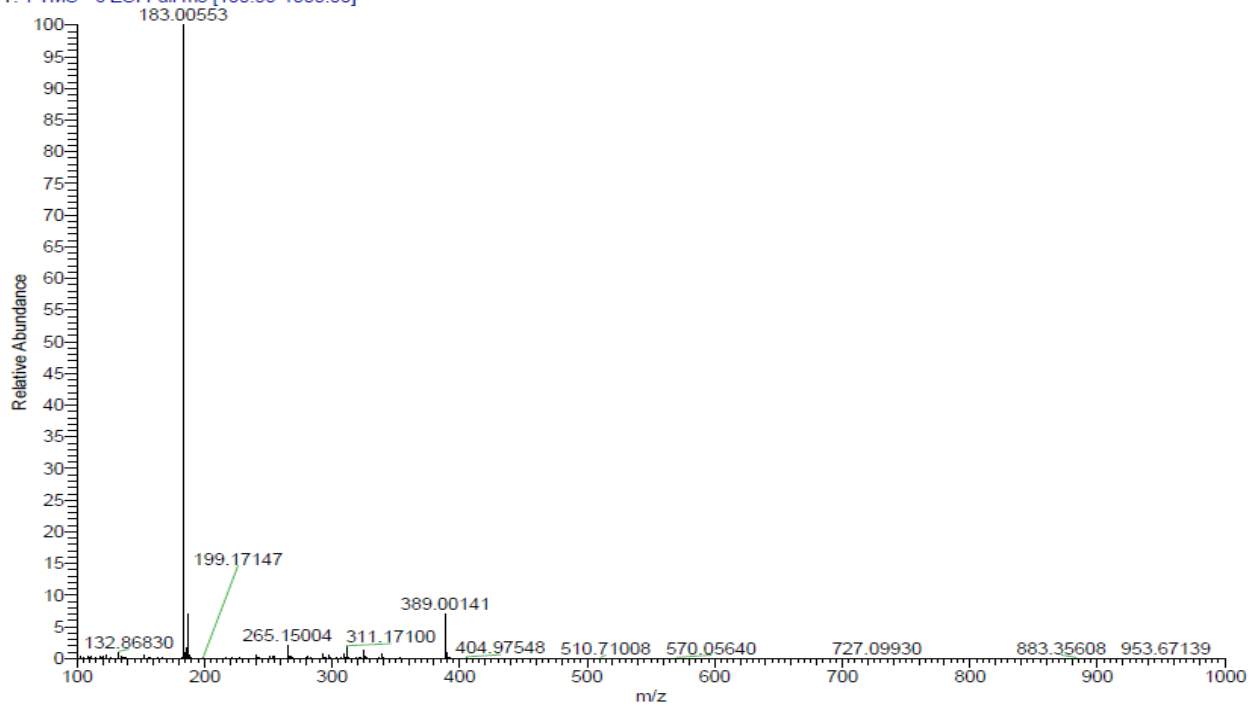


Figure S25: HRMS-ESI spectrum of complex 3b

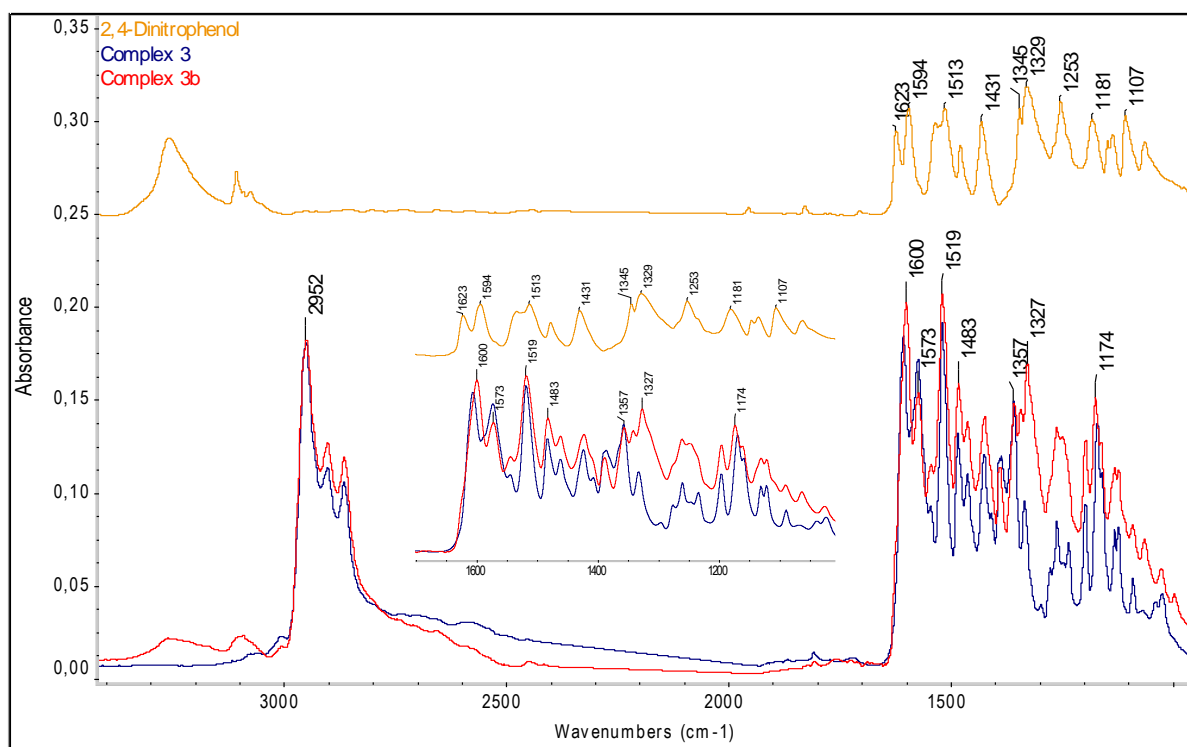


Figure S26: FT-IR spectra of complexes 3 and 3b

## 10. Characterization of complex 3d

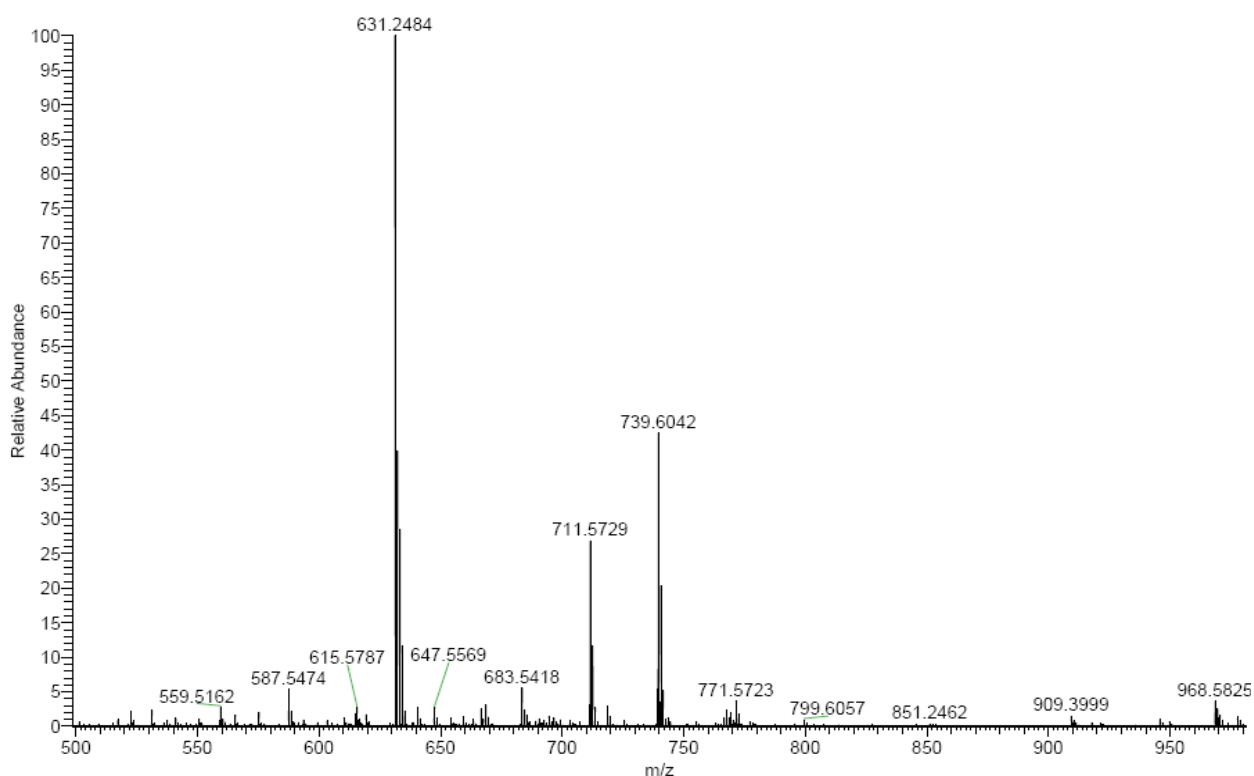


Figure S27: HRMS-ESI<sup>+</sup> spectrum of complex 3d

## 11. Crystal data of complex 2c

Crystal data for complex 2c:  $C_{50}H_{47}CoF_{10}N_2O_6$ ,  $M_r = 1020.83$ , triclinic,  $P\bar{1}$  (No 2),  $a = 13.6323$  (6) Å,  $b = 14.3118$  (6) Å,  $c = 14.4602$  (6) Å,  $\alpha = 76.884$  (2)°,  $\beta = 85.260$  (2)°,  $\gamma = 65.678$  (2)°;  $Z = 2$ ,  $D_x = 1.354$  Mg·m<sup>-3</sup>, dark red crystal of dimensions 0.40 × 0.31 × 0.18 mm, the multi-scan absorption correction was applied was ( $\mu = 0.43$  mm<sup>-1</sup>),  $T_{min} = 0.846$ ,  $T_{max} = 0.925$ ; 31019 diffraction collected ( $\theta_{max} = 27^\circ$ ), 10924 independent ( $R_{int} = 0.032$ ) and 8543 observed ( $I > 2\sigma(I)$ ). The refinement converged ( $\Delta/\sigma_{max} = 0.001$ ) to  $R = 0.046$  for observed reflections and  $wR(F^2) = 0.127$ ,  $GOF = 1.08$  for 634 parameters and all 10924 reflections. The final difference map displayed no peaks of chemical significance ( $\Delta\rho_{max} = 0.79$ ,  $\Delta\rho_{min} = -0.51$  e·Å<sup>-3</sup>)

### Crystal data

$C_{50}H_{47}CoF_{10}N_2O_6$	$Z = 2$
$M_r = 1020.83$	$F(000) = 1052$
Triclinic, $P\bar{1}$	$D_x = 1.354$ Mg m <sup>-3</sup>
$a = 13.6323$ (6) Å	Mo K $\alpha$ radiation, $\lambda = 0.71073$ Å
$b = 14.3118$ (6) Å	Cell parameters from 9942 reflections
$c = 14.4602$ (6) Å	$q = 2.7\text{--}27.0^\circ$
$\alpha = 76.884$ (2)°	$m = 0.43$ mm <sup>-1</sup>
$\beta = 85.260$ (2)°	$T = 150$ K
$\gamma = 65.678$ (2)°	Prism, dark red
$V = 2503.58$ (18) Å <sup>3</sup>	0.40 × 0.31 × 0.18 mm

### Data collection

Bruker APEX-II CCD diffractometer	10924 independent reflections
Radiation source: fine-focus sealed tube	8543 reflections with $I > 2\sigma(I)$
Graphite monochromator	$R_{\text{int}} = 0.032$
f and w scans	$q_{\text{max}} = 27.0^\circ$ , $q_{\text{min}} = 1.5^\circ$
Absorption correction: multi-scan SADABS V2012/1 (Bruker AXS Inc.)	$h = -17^{*}16$
$T_{\text{min}} = 0.846$ , $T_{\text{max}} = 0.925$	$k = -18^{*}13$
31019 measured reflections	$l = -18^{*}18$

### Refinement

Refinement on $F^2$	Primary atom site location: structure-invariant direct methods
Least-squares matrix: full	Secondary atom site location: difference Fourier map
$R[F^2 > 2\sigma(F^2)] = 0.046$	Hydrogen site location: inferred from neighbouring sites
$wR(F^2) = 0.127$	H atoms treated by a mixture of independent and constrained refinement
$S = 1.08$	$w = 1/[s^2(F_o^2) + (0.0703P)^2 + 0.2024P]$ where $P = (F_o^2 + 2F_c^2)/3$
10924 reflections	$(D/s)_{\text{max}} = 0.001$
634 parameters	$D\rho_{\text{max}} = 0.79 \text{ e } \text{\AA}^{-3}$
0 restraints	$D\rho_{\text{min}} = -0.51 \text{ e } \text{\AA}^{-3}$

### Special details

<p><i>Geometry.</i> All esds (except the esd in the dihedral angle between two l.s. planes) are estimated using the full covariance matrix. The cell esds are taken into account individually in the estimation of esds in distances, angles and torsion angles; correlations between esds in cell parameters are only used when they are defined by crystal symmetry. An approximate (isotropic) treatment of cell esds is used for estimating esds involving l.s. planes.</p>
<p><i>Refinement.</i> Refinement of <math>F^2</math> against ALL reflections. The weighted R-factor <math>wR</math> and goodness of fit <math>S</math> are based on <math>F^2</math>, conventional R-factors <math>R</math> are based on <math>F</math>, with <math>F</math> set to zero for negative <math>F^2</math>. The threshold expression of <math>F^2 &gt; 2\sigma(F^2)</math> is used only for calculating R-factors(gt) etc. and is not relevant to the choice of reflections for refinement. R-factors based on <math>F^2</math> are statistically about twice as large as those based on <math>F</math>, and R-factors based on ALL data will be even larger.</p>

### Geometric parameters ( $\text{\AA}$ , $^\circ$ ) for $2c$

Co1—O2	1.8607 (12)	C21—H21C	0.9800
Co1—N2	1.8626 (15)	C22—C23	1.416 (3)
Co1—O3	1.8807 (13)	C22—H22	0.9500
Co1—N1	1.9106 (15)	C23—C28	1.414 (3)
Co1—O1	1.9612 (13)	C23—C24	1.427 (3)
Co1—O5	1.9681 (13)	C24—C25	1.367 (3)

N1—C7	1.293 (2)	C24—H24	0.9500
N1—C1	1.418 (2)	C25—C26	1.402 (3)
N2—C22	1.307 (2)	C25—C33	1.532 (3)
N2—C6	1.417 (2)	C26—C27	1.383 (3)
O1—C9	1.386 (2)	C26—H26	0.9500
O1—H1	0.9638	C27—C28	1.432 (3)
O2—C28	1.320 (2)	C27—C29	1.528 (3)
O3—C37	1.231 (2)	C29—C32	1.533 (3)
O5—C44	1.242 (2)	C29—C30	1.535 (3)
O6—C44	1.251 (2)	C29—C31	1.541 (3)
O4—C37	1.220 (2)	C30—H30A	0.9800
C1—C2	1.394 (3)	C30—H30B	0.9800
C1—C6	1.399 (3)	C30—H30C	0.9800
C2—C3	1.373 (3)	C31—H31A	0.9800
C2—H2	0.9500	C31—H31B	0.9800
C3—C4	1.395 (3)	C31—H31C	0.9800
C3—H3	0.9500	C32—H32A	0.9800
C4—C5	1.386 (3)	C32—H32B	0.9800
C4—H4	0.9500	C32—H32C	0.9800
C5—C6	1.390 (3)	C33—C35	1.521 (3)
C5—H5	0.9500	C33—C36	1.524 (3)
C7—C8	1.437 (3)	C33—C34	1.533 (3)
C7—H7	0.9500	C34—H34A	0.9800
C8—C9	1.405 (3)	C34—H34B	0.9800
C8—C13	1.408 (3)	C34—H34C	0.9800
C9—C10	1.390 (3)	C35—H35A	0.9800
C10—C11	1.402 (3)	C35—H35B	0.9800
C10—C18	1.544 (3)	C35—H35C	0.9800
C11—C12	1.398 (3)	C36—H36A	0.9800
C11—H11	0.9500	C36—H36B	0.9800
C12—C13	1.371 (3)	C36—H36C	0.9800
C12—C14	1.536 (2)	C37—C38	1.549 (3)
C13—H13	0.9500	C38—C43	1.388 (3)
C14—C15	1.519 (3)	C38—C39	1.393 (3)
C14—C16	1.532 (3)	C39—F1	1.332 (2)
C14—C17	1.536 (3)	C39—C40	1.373 (3)
C15—H15A	0.9800	C40—F2	1.341 (3)
C15—H15B	0.9800	C40—C41	1.356 (3)
C15—H15C	0.9800	C41—F3	1.342 (3)
C16—H16A	0.9800	C41—C42	1.367 (4)
C16—H16B	0.9800	C42—F4	1.345 (3)
C16—H16C	0.9800	C42—C43	1.376 (4)

C17—H17A	0.9800	C43—F5	1.330 (3)
C17—H17B	0.9800	C44—C45	1.511 (3)
C17—H17C	0.9800	C45—C50	1.379 (3)
C18—C21	1.527 (3)	C45—C46	1.388 (3)
C18—C19	1.537 (3)	C46—F6	1.330 (2)
C18—C20	1.544 (3)	C46—C47	1.382 (3)
C19—H19A	0.9800	C47—F7	1.343 (3)
C19—H19B	0.9800	C47—C48	1.371 (3)
C19—H19C	0.9800	C48—F8	1.339 (3)
C20—H20A	0.9800	C48—C49	1.383 (3)
C20—H20B	0.9800	C49—F9	1.337 (3)
C20—H20C	0.9800	C49—C50	1.373 (3)
C21—H21A	0.9800	C50—F10	1.347 (2)
C21—H21B	0.9800		
O2—Co1—N2	96.24 (6)	H21B—C21—H21C	109.5
O2—Co1—O3	93.27 (6)	N2—C22—C23	125.94 (18)
N2—Co1—O3	97.50 (7)	N2—C22—H22	117.0
O2—Co1—N1	178.40 (6)	C23—C22—H22	117.0
N2—Co1—N1	85.28 (6)	C28—C23—C22	123.10 (17)
O3—Co1—N1	86.03 (6)	C28—C23—C24	120.71 (17)
O2—Co1—O1	85.97 (5)	C22—C23—C24	116.16 (18)
N2—Co1—O1	176.27 (6)	C25—C24—C23	121.50 (19)
O3—Co1—O1	85.35 (6)	C25—C24—H24	119.2
N1—Co1—O1	92.54 (6)	C23—C24—H24	119.2
O2—Co1—O5	88.09 (6)	C24—C25—C26	116.31 (17)
N2—Co1—O5	85.28 (6)	C24—C25—C33	123.40 (19)
O3—Co1—O5	176.75 (6)	C26—C25—C33	120.26 (17)
N1—Co1—O5	92.54 (6)	C27—C26—C25	125.60 (18)
O1—Co1—O5	91.81 (5)	C27—C26—H26	117.2
C7—N1—C1	121.67 (16)	C25—C26—H26	117.2
C7—N1—Co1	125.03 (13)	C26—C27—C28	117.46 (18)
C1—N1—Co1	112.67 (11)	C26—C27—C29	121.87 (17)
C22—N2—C6	121.28 (16)	C28—C27—C29	120.67 (16)
C22—N2—Co1	123.47 (13)	O2—C28—C23	123.26 (16)
C6—N2—Co1	113.79 (12)	O2—C28—C27	118.91 (17)
C9—O1—Co1	125.48 (11)	C23—C28—C27	117.83 (16)
C9—O1—H1	106.9	C27—C29—C32	109.69 (17)
Co1—O1—H1	101.6	C27—C29—C30	111.58 (17)
C28—O2—Co1	125.55 (12)	C32—C29—C30	107.46 (19)
C37—O3—Co1	126.31 (13)	C27—C29—C31	110.37 (18)
C44—O5—Co1	126.20 (13)	C32—C29—C31	110.71 (18)

C2—C1—C6	119.99 (17)	C30—C29—C31	106.97 (17)
C2—C1—N1	126.42 (16)	C29—C30—H30A	109.5
C6—C1—N1	113.58 (16)	C29—C30—H30B	109.5
C3—C2—C1	119.58 (17)	H30A—C30—H30B	109.5
C3—C2—H2	120.2	C29—C30—H30C	109.5
C1—C2—H2	120.2	H30A—C30—H30C	109.5
C2—C3—C4	120.47 (18)	H30B—C30—H30C	109.5
C2—C3—H3	119.8	C29—C31—H31A	109.5
C4—C3—H3	119.8	C29—C31—H31B	109.5
C5—C4—C3	120.58 (19)	H31A—C31—H31B	109.5
C5—C4—H4	119.7	C29—C31—H31C	109.5
C3—C4—H4	119.7	H31A—C31—H31C	109.5
C4—C5—C6	119.07 (18)	H31B—C31—H31C	109.5
C4—C5—H5	120.5	C29—C32—H32A	109.5
C6—C5—H5	120.5	C29—C32—H32B	109.5
C5—C6—C1	120.21 (17)	H32A—C32—H32B	109.5
C5—C6—N2	125.32 (16)	C29—C32—H32C	109.5
C1—C6—N2	114.46 (16)	H32A—C32—H32C	109.5
N1—C7—C8	127.41 (17)	H32B—C32—H32C	109.5
N1—C7—H7	116.3	C35—C33—C36	109.5 (2)
C8—C7—H7	116.3	C35—C33—C25	111.53 (18)
C9—C8—C13	118.90 (17)	C36—C33—C25	108.03 (17)
C9—C8—C7	124.91 (16)	C35—C33—C34	107.33 (19)
C13—C8—C7	116.07 (16)	C36—C33—C34	108.7 (2)
O1—C9—C10	119.91 (16)	C25—C33—C34	111.67 (17)
O1—C9—C8	118.98 (16)	C33—C34—H34A	109.5
C10—C9—C8	121.10 (16)	C33—C34—H34B	109.5
C9—C10—C11	116.93 (17)	H34A—C34—H34B	109.5
C9—C10—C18	123.06 (16)	C33—C34—H34C	109.5
C11—C10—C18	119.99 (17)	H34A—C34—H34C	109.5
C12—C11—C10	124.08 (18)	H34B—C34—H34C	109.5
C12—C11—H11	118.0	C33—C35—H35A	109.5
C10—C11—H11	118.0	C33—C35—H35B	109.5
C13—C12—C11	116.90 (17)	H35A—C35—H35B	109.5
C13—C12—C14	121.33 (17)	C33—C35—H35C	109.5
C11—C12—C14	121.55 (17)	H35A—C35—H35C	109.5
C12—C13—C8	122.02 (17)	H35B—C35—H35C	109.5
C12—C13—H13	119.0	C33—C36—H36A	109.5
C8—C13—H13	119.0	C33—C36—H36B	109.5
C15—C14—C16	107.67 (17)	H36A—C36—H36B	109.5
C15—C14—C12	112.47 (16)	C33—C36—H36C	109.5
C16—C14—C12	110.87 (16)	H36A—C36—H36C	109.5

C15—C14—C17	109.65 (19)	H36B—C36—H36C	109.5
C16—C14—C17	109.28 (19)	O4—C37—O3	129.4 (2)
C12—C14—C17	106.88 (16)	O4—C37—C38	117.84 (19)
C14—C15—H15A	109.5	O3—C37—C38	112.80 (16)
C14—C15—H15B	109.5	C43—C38—C39	115.0 (2)
H15A—C15—H15B	109.5	C43—C38—C37	121.70 (19)
C14—C15—H15C	109.5	C39—C38—C37	123.28 (18)
H15A—C15—H15C	109.5	F1—C39—C40	115.30 (19)
H15B—C15—H15C	109.5	F1—C39—C38	122.01 (19)
C14—C16—H16A	109.5	C40—C39—C38	122.7 (2)
C14—C16—H16B	109.5	F2—C40—C41	119.4 (2)
H16A—C16—H16B	109.5	F2—C40—C39	120.3 (2)
C14—C16—H16C	109.5	C41—C40—C39	120.4 (2)
H16A—C16—H16C	109.5	F3—C41—C40	120.4 (2)
H16B—C16—H16C	109.5	F3—C41—C42	120.4 (2)
C14—C17—H17A	109.5	C40—C41—C42	119.2 (2)
C14—C17—H17B	109.5	F4—C42—C41	120.0 (2)
H17A—C17—H17B	109.5	F4—C42—C43	119.7 (2)
C14—C17—H17C	109.5	C41—C42—C43	120.3 (2)
H17A—C17—H17C	109.5	F5—C43—C42	116.4 (2)
H17B—C17—H17C	109.5	F5—C43—C38	121.2 (2)
C21—C18—C19	108.16 (19)	C42—C43—C38	122.4 (2)
C21—C18—C10	112.01 (16)	O5—C44—O6	126.82 (18)
C19—C18—C10	108.82 (17)	O5—C44—C45	117.33 (17)
C21—C18—C20	106.71 (18)	O6—C44—C45	115.84 (17)
C19—C18—C20	110.42 (18)	C50—C45—C46	117.34 (19)
C10—C18—C20	110.69 (17)	C50—C45—C44	120.91 (18)
C18—C19—H19A	109.5	C46—C45—C44	121.66 (18)
C18—C19—H19B	109.5	F6—C46—C47	118.35 (19)
H19A—C19—H19B	109.5	F6—C46—C45	120.36 (18)
C18—C19—H19C	109.5	C47—C46—C45	121.3 (2)
H19A—C19—H19C	109.5	F7—C47—C48	120.2 (2)
H19B—C19—H19C	109.5	F7—C47—C46	119.9 (2)
C18—C20—H20A	109.5	C48—C47—C46	119.8 (2)
C18—C20—H20B	109.5	F8—C48—C47	120.0 (2)
H20A—C20—H20B	109.5	F8—C48—C49	120.0 (2)
C18—C20—H20C	109.5	C47—C48—C49	120.1 (2)
H20A—C20—H20C	109.5	F9—C49—C50	120.7 (2)
H20B—C20—H20C	109.5	F9—C49—C48	120.1 (2)
C18—C21—H21A	109.5	C50—C49—C48	119.2 (2)
C18—C21—H21B	109.5	F10—C50—C49	117.7 (2)
H21A—C21—H21B	109.5	F10—C50—C45	119.99 (18)

C18—C21—H21C	109.5	C49—C50—C45	122.3 (2)
H21A—C21—H21C	109.5		
N2—Co1—N1—C7	-169.60 (16)	C22—C23—C24—C25	-178.53 (18)
O3—Co1—N1—C7	-71.73 (16)	C23—C24—C25—C26	-4.4 (3)
O1—Co1—N1—C7	13.43 (16)	C23—C24—C25—C33	173.57 (18)
O5—Co1—N1—C7	105.35 (16)	C24—C25—C26—C27	2.8 (3)
N2—Co1—N1—C1	1.35 (12)	C33—C25—C26—C27	-175.24 (19)
O3—Co1—N1—C1	99.23 (12)	C25—C26—C27—C28	3.7 (3)
O1—Co1—N1—C1	-175.62 (12)	C25—C26—C27—C29	-176.90 (19)
O5—Co1—N1—C1	-83.69 (12)	Co1—O2—C28—C23	7.2 (3)
O2—Co1—N2—C22	15.73 (16)	Co1—O2—C28—C27	-172.65 (13)
O3—Co1—N2—C22	109.87 (15)	C22—C23—C28—O2	5.1 (3)
N1—Co1—N2—C22	-164.78 (16)	C24—C23—C28—O2	-172.83 (17)
O5—Co1—N2—C22	-71.82 (15)	C22—C23—C28—C27	-175.09 (17)
O2—Co1—N2—C6	-177.93 (12)	C24—C23—C28—C27	7.0 (3)
O3—Co1—N2—C6	-83.79 (13)	C26—C27—C28—O2	171.47 (17)
N1—Co1—N2—C6	1.57 (12)	C29—C27—C28—O2	-7.9 (3)
O5—Co1—N2—C6	94.52 (12)	C26—C27—C28—C23	-8.4 (3)
O2—Co1—O1—C9	152.85 (14)	C29—C27—C28—C23	172.23 (18)
O3—Co1—O1—C9	59.24 (14)	C26—C27—C29—C32	123.1 (2)
N1—Co1—O1—C9	-26.57 (14)	C28—C27—C29—C32	-57.5 (2)
O5—Co1—O1—C9	-119.19 (14)	C26—C27—C29—C30	4.1 (3)
N2—Co1—O2—C28	-15.10 (15)	C28—C27—C29—C30	-176.49 (18)
O3—Co1—O2—C28	-113.02 (15)	C26—C27—C29—C31	-114.7 (2)
O1—Co1—O2—C28	161.89 (15)	C28—C27—C29—C31	64.7 (2)
O5—Co1—O2—C28	69.94 (14)	C24—C25—C33—C35	132.3 (2)
O2—Co1—O3—C37	38.60 (17)	C26—C25—C33—C35	-49.9 (3)
N2—Co1—O3—C37	-58.15 (17)	C24—C25—C33—C36	-107.3 (2)
N1—Co1—O3—C37	-142.85 (17)	C26—C25—C33—C36	70.5 (3)
O1—Co1—O3—C37	124.28 (17)	C24—C25—C33—C34	12.2 (3)
O2—Co1—O5—C44	73.86 (15)	C26—C25—C33—C34	-169.98 (19)
N2—Co1—O5—C44	170.29 (15)	Co1—O3—C37—O4	14.5 (3)
N1—Co1—O5—C44	-104.66 (15)	Co1—O3—C37—C38	-165.82 (12)
O1—Co1—O5—C44	-12.04 (15)	O4—C37—C38—C43	-1.3 (3)
C7—N1—C1—C2	-11.7 (3)	O3—C37—C38—C43	178.9 (2)
Co1—N1—C1—C2	177.03 (16)	O4—C37—C38—C39	176.9 (2)
C7—N1—C1—C6	167.26 (17)	O3—C37—C38—C39	-2.9 (3)
Co1—N1—C1—C6	-4.0 (2)	C43—C38—C39—F1	179.1 (2)
C6—C1—C2—C3	-0.9 (3)	C37—C38—C39—F1	0.8 (4)
N1—C1—C2—C3	177.98 (18)	C43—C38—C39—C40	-0.3 (4)
C1—C2—C3—C4	-1.5 (3)	C37—C38—C39—C40	-178.6 (2)

C2—C3—C4—C5	1.5 (3)	F1—C39—C40—F2	0.7 (4)
C3—C4—C5—C6	0.9 (3)	C38—C39—C40—F2	-179.9 (2)
C4—C5—C6—C1	-3.3 (3)	F1—C39—C40—C41	-178.3 (3)
C4—C5—C6—N2	175.50 (18)	C38—C39—C40—C41	1.1 (4)
C2—C1—C6—C5	3.3 (3)	F2—C40—C41—F3	-1.1 (4)
N1—C1—C6—C5	-175.69 (17)	C39—C40—C41—F3	177.9 (3)
C2—C1—C6—N2	-175.62 (16)	F2—C40—C41—C42	-179.8 (3)
N1—C1—C6—N2	5.4 (2)	C39—C40—C41—C42	-0.8 (5)
C22—N2—C6—C5	-16.5 (3)	F3—C41—C42—F4	1.0 (5)
Co1—N2—C6—C5	176.85 (16)	C40—C41—C42—F4	179.7 (3)
C22—N2—C6—C1	162.40 (17)	F3—C41—C42—C43	-178.9 (3)
Co1—N2—C6—C1	-4.3 (2)	C40—C41—C42—C43	-0.3 (5)
C1—N1—C7—C8	-171.16 (18)	F4—C42—C43—F5	0.7 (5)
Co1—N1—C7—C8	-1.0 (3)	C41—C42—C43—F5	-179.3 (3)
N1—C7—C8—C9	-5.9 (3)	F4—C42—C43—C38	-178.9 (3)
N1—C7—C8—C13	170.04 (19)	C41—C42—C43—C38	1.1 (5)
Co1—O1—C9—C10	-154.02 (14)	C39—C38—C43—F5	179.7 (3)
Co1—O1—C9—C8	26.6 (2)	C37—C38—C43—F5	-2.0 (4)
C13—C8—C9—O1	176.43 (16)	C39—C38—C43—C42	-0.8 (4)
C7—C8—C9—O1	-7.7 (3)	C37—C38—C43—C42	177.5 (3)
C13—C8—C9—C10	-2.9 (3)	Co1—O5—C44—O6	13.7 (3)
C7—C8—C9—C10	172.95 (18)	Co1—O5—C44—C45	-166.30 (12)
O1—C9—C10—C11	-176.71 (17)	O5—C44—C45—C50	-125.8 (2)
C8—C9—C10—C11	2.6 (3)	O6—C44—C45—C50	54.2 (3)
O1—C9—C10—C18	5.2 (3)	O5—C44—C45—C46	57.8 (3)
C8—C9—C10—C18	-175.50 (18)	O6—C44—C45—C46	-122.2 (2)
C9—C10—C11—C12	-1.0 (3)	C50—C45—C46—F6	-179.03 (19)
C18—C10—C11—C12	177.15 (18)	C44—C45—C46—F6	-2.5 (3)
C10—C11—C12—C13	-0.3 (3)	C50—C45—C46—C47	-0.5 (3)
C10—C11—C12—C14	-174.89 (18)	C44—C45—C46—C47	175.95 (19)
C11—C12—C13—C8	0.0 (3)	F6—C46—C47—F7	-0.5 (3)
C14—C12—C13—C8	174.64 (18)	C45—C46—C47—F7	-179.0 (2)
C9—C8—C13—C12	1.5 (3)	F6—C46—C47—C48	178.5 (2)
C7—C8—C13—C12	-174.69 (18)	C45—C46—C47—C48	0.0 (4)
C13—C12—C14—C15	164.47 (19)	F7—C47—C48—F8	-0.5 (4)
C11—C12—C14—C15	-21.2 (3)	C46—C47—C48—F8	-179.4 (2)
C13—C12—C14—C16	43.9 (3)	F7—C47—C48—C49	179.7 (2)
C11—C12—C14—C16	-141.8 (2)	C46—C47—C48—C49	0.8 (4)
C13—C12—C14—C17	-75.1 (2)	F8—C48—C49—F9	-0.1 (4)
C11—C12—C14—C17	99.2 (2)	C47—C48—C49—F9	179.7 (2)
C9—C10—C18—C21	177.2 (2)	F8—C48—C49—C50	179.3 (2)
C11—C10—C18—C21	-0.8 (3)	C47—C48—C49—C50	-0.9 (4)

C9—C10—C18—C19	57.7 (3)	F9—C49—C50—F10	-1.5 (3)
C11—C10—C18—C19	-120.3 (2)	C48—C49—C50—F10	179.1 (2)
C9—C10—C18—C20	-63.8 (3)	F9—C49—C50—C45	179.7 (2)
C11—C10—C18—C20	118.1 (2)	C48—C49—C50—C45	0.3 (4)
C6—N2—C22—C23	-174.40 (17)	C46—C45—C50—F10	-178.40 (18)
Co1—N2—C22—C23	-9.0 (3)	C44—C45—C50—F10	5.1 (3)
N2—C22—C23—C28	-4.0 (3)	C46—C45—C50—C49	0.4 (3)
N2—C22—C23—C24	173.98 (18)	C44—C45—C50—C49	-176.1 (2)
C28—C23—C24—C25	-0.5 (3)		

*Hydrogen-bond geometry (Å, °) for 2c*

<i>D—H...A</i>	<i>D—H</i>	<i>H...A</i>	<i>D...A</i>	<i>D—H...A</i>
O1—H1...O6	0.96	1.50	2.4418 (19)	165

Crystallographic data was collected on Nonius KappaCCD diffractometer equipped with Bruker APEX-II CCD detector by monochromatized MoK $\alpha$  radiation ( $\lambda = 0.71073$  Å) at the temperature of 150(2) K. The structure was solved by direct methods (SHELXS)<sup>1</sup> and refined by full matrix least squares based on  $F^2$  (SHELXL97)<sup>1</sup>. The hydrogen atoms on carbon were calculated into idealized positions and were refined as fixed (riding model) with assigned temperature factors  $H_{iso}(H) = 1.2 U_{eq}(\text{pivot atom})$  or  $1.5 U_{eq}$  for methyl moiety.

The hydrogen in –OH moiety was found on difference Fourier map and fixed during refinement with assigned temperature factors  $H_{iso}(H) = 1.2 U_{eq}(O(6))$ .

To improved the resolution of the complex PLATON<sup>2</sup>/ SQUEEZE procedure was used to correct the data for the presence of the disordered dichlormethane solvent. One potential solvent cavity with volume of  $292\text{Å}^3$  was found at special position of inversion. 57 electrons worth of scattering were located in the void, highest peak corresponds to electron density  $2.1 \text{ e/Å}^3$ .

1. Sheldrick, G.M. (2008). *Acta Cryst.* **A64**, 112-122
2. Spek, A.L. (2009). *Acta Cryst.* **D65**, 148-155